

Review

# Development of All-Solid-State Li-Ion Batteries: From Key Technical Areas to Commercial Use

Constantin Bubulinca <sup>1,\*</sup>, Natalia E. Kazantseva <sup>1</sup>, Viera Pechancova <sup>1,2</sup> , Nikhitha Joseph <sup>1</sup>, Haojie Fei <sup>1</sup>, Mariana Venher <sup>1</sup>, Anna Ivanichenko <sup>1</sup> and Petr Saha <sup>1,2</sup>

<sup>1</sup> Centre of Polymer Systems, Tomas Bata University in Zlín, Tr. T. Bati 5678, 760 01 Zlín, Czech Republic

<sup>2</sup> University Institute, Tomas Bata University in Zlín, Nad Ovčímou IV 3685, 760 01 Zlín, Czech Republic

\* Correspondence: bubulinca@utb.cz

**Abstract:** Innovation in the design of Li-ion rechargeable batteries is necessary to overcome safety concerns and meet energy demands. In this regard, a new generation of Li-ion batteries (LIBs) in the form of all-solid-state batteries (ASSBs) has been developed, attracting a great deal of attention for their high-energy density and excellent mechanical-electrochemical stability. This review describes the current state of research and development on ASSB technology. To this end, study of the literature and patents as well as market analysis over the last two decades were carried out, highlighting how scientific achievements have informed the application of commercially profitable ASSBs. Analyzing the patents registered over the past 20 years revealed that the number of them had increased exponentially—from only few per year in early 2000 to more than 342 in 2020. Published literature and patents on the topic declare a solid-state electrolyte (SSE) to be the main component of ASSBs, and most patented examples are referred to as solid inorganic electrolytes (SIEs), followed by solid polymer electrolytes (SPEs) and solid hybrid electrolytes (SHEs) in popularity. Investigation of company websites, social media profiles, reports, and academic publications identified 93 companies associated with ASSBs. A list of leading businesses in the solid-state battery sector was compiled, out of which 36 provided information on the ASSB units in their product portfolio for detailed analysis.

**Keywords:** all-solid-state batteries; solid-state electrolyte; patent analysis; review of the ASSB market



**Citation:** Bubulinca, C.; Kazantseva, N.E.; Pechancova, V.; Joseph, N.; Fei, H.; Venher, M.; Ivanichenko, A.; Saha, P. Development of All-Solid-State Li-Ion Batteries: From Key Technical Areas to Commercial Use. *Batteries* **2023**, *9*, 157. <https://doi.org/10.3390/batteries9030157>

Academic Editor: Atsushi Nagai

Received: 15 December 2022

Revised: 14 February 2023

Accepted: 24 February 2023

Published: 1 March 2023



**Copyright:** © 2023 by the authors. Licensee MDPI, Basel, Switzerland. This article is an open access article distributed under the terms and conditions of the Creative Commons Attribution (CC BY) license (<https://creativecommons.org/licenses/by/4.0/>).

## 1. Introduction

In recent years, new types of batteries have been launched that make use of lithium, the lightest element in the periodic table. Their properties differ in relation to size, shape, voltage, and the reactions employed. The lithium-ion battery market is changing rapidly, worth 34.2 billion USD in 2020, it is expected to rise to 182.53 billion USD in 2030, driven by anticipated growth in the electric vehicle (EV) market [1]. Advancements in the development of materials and electrode engineering have led to a reduction in lithium-ion battery costs by 90% per unit, and an increase in gravimetric energy density from an initial level of ca 90 Wh kg<sup>-1</sup> to 250 Wh kg<sup>-1</sup>. A lithium-ion battery provides a high voltage window of around 4 V, resulting in greater volumetric and gravimetric energy densities than other rechargeable options, making it the technology of choice for portable electronics and power tools [2]. With regard to all-electric, plug-in and hybrid vehicles, the technologies applied in them necessitate the construction and use of rechargeable lithium-ion batteries. An alternative solution of a dual-ion battery exists. Fabricated by cation intercalation, examples include an aluminum-graphite battery with high levels of reversibility and energy density [3], and a calcium-ion battery capable of working stably at room temperature, which has a novel cell configuration with graphite as the cathode and tin foil as both the anode and the current collector [4].

Numerous review papers have been published on the current state-of-the-art of LIBs [5,6], covering aspects related to safety concerns [7] and factors affecting their performance at low temperature [8–10].

This work combines analysis of the major technical challenges faced in the development of all-solid-state lithium-ion batteries with evaluation of related advancement in the global market, based on patents, prototypes, and products presented by companies, research centers and universities.

### Brief history of LIBs

Research on lithium-ion batteries (LIBs) began during the oil crisis in the 1970s, when scientists pondered options for alternative energy sources and the potential of rechargeable devices. Stanley Whittingham, a chemist at Exxon mobile, devised a novel battery design with titanium disulfide as the cathode and lithium metal as the anode, which could be charged in a short period of time (Figure 1a). It was not successful, however, due to the thermal runaway evident in early tests. An engineering professor and physicist, John B. Goodenough from the University of Texas in Austin, advanced it by swapping out the titanium disulfide cathode for lithium cobalt oxide (LCO), thereby doubling the energy capacity of the battery (Figure 1b) [11]. Five years later, Akira Yoshino from Meijo University in Nagoya, Japan, applied a carbonaceous material instead of the lithium metal anode, which proved ground-breaking, as it was the first prototype of a lithium-ion battery without lithium metal (Figure 1c). For developing this “rechargeable technology”, the three aforementioned scientists shared the Nobel Prize in 2019.

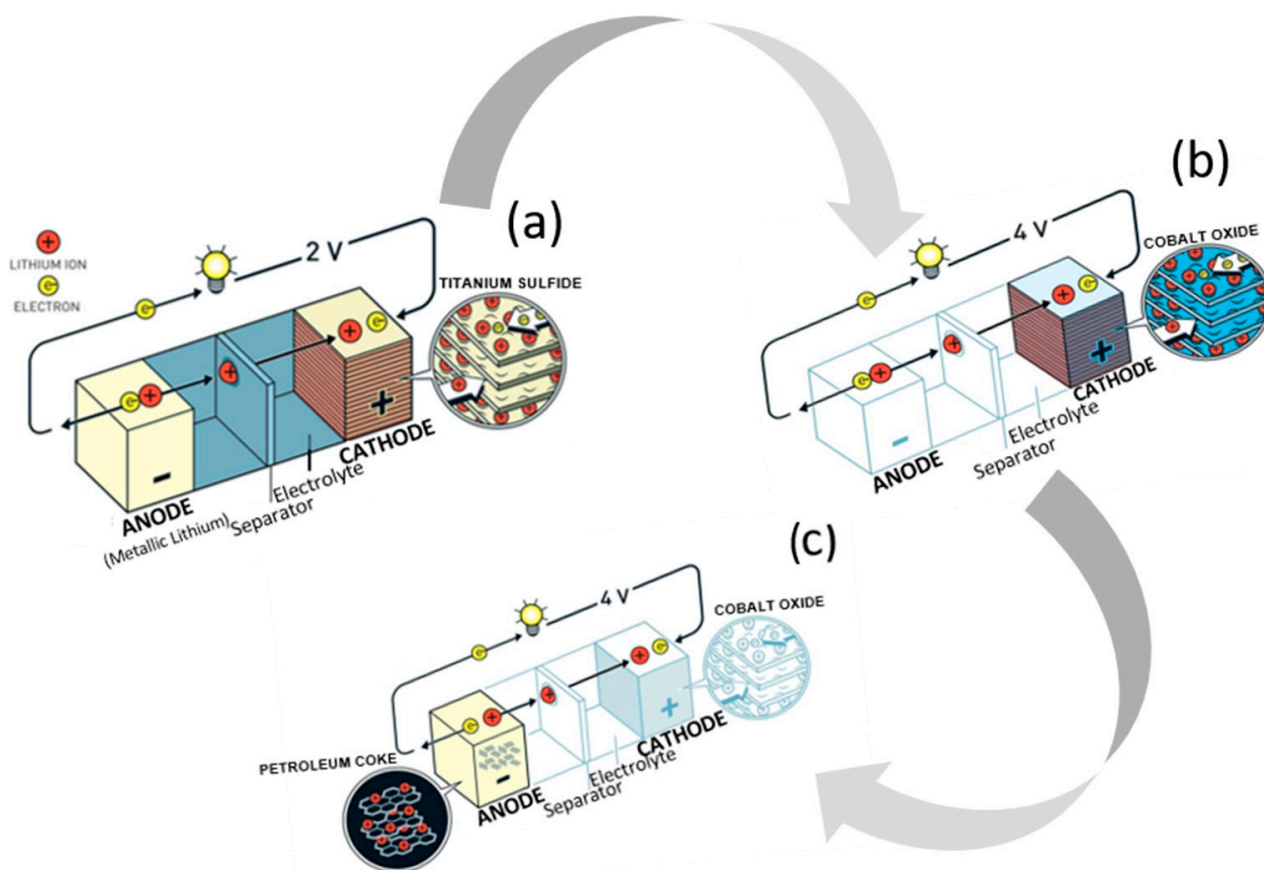


**Figure 1.** Battery designs by Whittingham (a), Goodenough (b), and Yoshino (c).

In 1997, a research team led by Goodenough introduced the cathode material of lithium iron phosphate (LFP), an alternative to LCO, since CO is high in toxicity and more expensive. LFP has the advantages of low material cost, nontoxicity, a 3.5 V operating voltage (in contrast with Li/Li+), a considerable theoretical specific capacity of 170 mAh g<sup>-1</sup>, high stability, and prolonged cycle life. Compared to other cathode materials, though, the electronic conductivity of the LFP cathode is limited to 10<sup>-9</sup> to 10<sup>-10</sup> S cm<sup>-1</sup> [12,13]. Other drawbacks include a poor ion diffusion rate, low tap density, and unacceptable electrochem-

ical performance at low temperature, limiting its further development [14–16]. A layered cathode material was proposed later, such as the combination of nickel, manganese, and cobalt ( $\text{LiNi}_{1-x-y}\text{Co}_x\text{Mn}_y\text{O}_2$ ; referred to as the NMC type of cathode), which boasts high specific capacity, low internal resistance, and heightened safety. Forms of NMC cathode with less cobalt content (e.g., NMC811, NMC442, NMC532) have garnered attention as cheaper options, and a great deal of research has been invested in developing cobalt-free alternatives. Comparing two designs capable of delivering 4.3 V, the greater amount of nickel in a cathode such as NMC811 facilitates a higher specific capacity of  $200 \text{ mAh g}^{-1}$  than NMC532 ( $160 \text{ mAh g}^{-1}$ ), versus Li/Li+ configurations. The increased level of Ni content in the cathode raises the reactivity of the cathode, however, due to the instability of the nickel ion with the liquid organic electrolyte, resulting in two-times the extent of moisture. This is why nickel-rich cathode materials need an additional electrode coating to prevent degradation during operation at high temperature [17,18].

Besides LIBs, a step-change in energy storage is the appeal of technologies that differ from Li-ion-based systems. Lithium-air (Li-air) and lithium-sulfur (Li-S) are theoretically capable of providing the kind of the performance required for the future. Aqueous and non-aqueous Li-air batteries were first described in the literature in [19] and [20,21] respectively. The concept of electrochemical energy conversion and storage, employing sulfur as the cathode in an alkali metal anode battery date back to at least 1960 [22]. Reactions at the cathode (the positive electrode) in Li-air and Li-S cells involve the reversible reduction of  $\text{O}_2$  and S, respectively, and are fundamentally different from those in Li-ion cells. Although theoretically the energy densities of Li-air and Li-S cells are high (Table 1), numerous issues need to be addressed prior to shifting the technology from theory to practice [23].

**Table 1.** Theoretical energy storage for LIBs.

Battery Chemistry	Cell Potential/V	Theoretical Specific Energy/Wh $\text{kg}^{-1}$
$\text{Li-S}_2\text{Li} + \text{S} = \text{Li}_2\text{S}$	2.2	2567
Li-air (non-aqueous) $2\text{Li} + \text{O}_2 = \text{Li}_2\text{O}_2$	3.0	3505
Li-air (aqueous) $2\text{Li} + \frac{1}{2}\text{O}_2 + \text{H}_2\text{O} = 2\text{LiOH}$	3.2	3582
Contemporary Li-ion $0.5\text{C}_6\text{Li} + \text{Li}_{0.5}\text{CoO}_2 = 3\text{C} + \text{LiCoO}_2$	3.8	387

A shuttle effect reported for lithium polysulfide (LiPSs) and slow sulfur reaction kinetics, caused by multi-step phase transitions, severely limit the practical application of Li-S batteries. These limitations can be overcome, though, by adopting a facile hydrothermal method and performing defect engineering to synthesize a cocklebur-like sulfur host with a  $\text{TiO}_2\text{-VO}_x$  heterostructure (CTVHs) in the production of long-life Li-S batteries [24]. Heterostructures have the potential to aid the development of new Li-S batteries or other energy storage systems, and could find widespread application in various interface control solutions.

### 1.1. Theoretical Aspects of Li-Ion Battery Technology

#### 1.1.1. Key Parameters of LIB Development

For the large-scale applicability of LIBs, such as in EVs and a smart grid arrangement, it is necessary to consider several factors. Putting LIBs in EVs, beyond energy-related concerns, means addressing several matters including cost, cycle life, safety, and environmental impact. In a smart grid setting, the related cost, safety, and life cycle are more important than energy density [25]. Modern LIBs are limited to a gravimetric energy density of  $<250 \text{ Wh kg}^{-1}$  and volumetric energy density of  $<650 \text{ Wh L}^{-1}$ ; an increase in these is anticipated of up to  $\sim 500 \text{ Wh kg}^{-1}$  and  $>1000 \text{ Wh L}^{-1}$ , respectively. Such performance parameters largely depend on the properties of the anode, cathode and electrolyte materials employed in the battery system, the given environment and intended use.

### 1.1.2. Solid Electrolyte Interface (SEI) Formation

Cell reactions that pose a challenge to LIB technology include the occurrence of a solid electrolyte interphase (SEI), electrolyte flammability, the dissolution of electrodes, and dendrite growth [26]. The formation of SEI in an advanced rechargeable battery system arises when such a battery is operated beyond the thermodynamic stability window of the electrolyte [27]. The interphase stems from the sacrificial decomposition of electrolytic components, such as solvent, salts, and additives, resulting in the formation of a thin film which separates the electrolyte from the electrode [28]. It has been proven that the composition of such an SEI is vital to superior performance of LIBs [29]. Nevertheless, lithium ions are consumed in the presence of an excessive SEI layer during delithiation, leading to capacity fade, a rise in impedance and creation of a barrier at the anode/electrolyte interface [30–33]. Decomposition of formed SEI also initiates a chain of reactions, and further results in thermal runaway of the LIB [30].

### 1.1.3. Safety Concerns

Another critical concern about LIBs is that of safety [34], and three main categories exist: (1) the reactivity of the material under conditions of abuse; (2) flammability of the electrolyte; and (3) the toxicity of the substance if released into the environment through a crack in the cell package [35]. Reactions inside the battery that will result in thermal runaway of the system are classified as anode–electrolyte, cathode–electrolyte, and cathode–anode reactions. Commonly used organic electrolytes have a favorable operating voltage window, yet under extreme conditions of temperature and voltage they may react with the electrodes and release a significant amount of heat and gas, effecting damage to other materials or failure of the same inside the battery [36]. Anode–electrolyte reactions are known to initiate a rise in heat production, while cathode–electrolyte and anode–cathode reactions trigger a combustion process; the latter only arising when a considerable amount of heat is produced [37,38]. Such combustibility of a carbonate electrolyte polymer in batteries, leading to thermal runaway, is instigated through mechanical or thermal stress, dendrite formation, decomposition of the electrolyte, and charging issues related to electrochemical abuse [39]. During abnormal charging conditions, such as overcharging, lithium is continuously eliminated on the cathode side, inducing breakdown of the cathode and oxygen evolution. Further effects comprise oxidation of organic solvents in the system and the intense generation of heat. Moreover, excessive deposition of lithium at the anode side initiates the formation of dendrites, while the reaction of such deposited lithium and the carbonate solvent produces a huge amount of heat and gas. Very small flash points are associated with the decomposition of common lithium salt LiPF<sub>6</sub> and the oxidation of carbonate solvents, e.g., ethylene carbonate (EC), propylene carbonate (PC), dimethyl carbonate (DMC), ethyl methyl carbonate (EMC), diethyl carbonate (DEC), and dimethyl carbonate (DME), which can be easily triggered under a state of high voltage or temperature. Should the temperature of the battery system go up, the LiPF<sub>6</sub> salt thermally decomposes to PF<sub>5</sub> before the solvents decompose. This PF<sub>5</sub> is a strong Lewis acid highly reactive with organic solvents, and such a reaction could encourage the thermal decomposition of carbonate-based solvents [40–42]. In addition, the unusual rise in temperature and generation of heat initiates side reactions such as breakdown of the SEI layer or destruction of the separator, which constitute causes of thermal runaway of the battery system [43–45]. In the case of EVs, a primary issue relates to the size of the battery, namely a decrease in the ratio between the thermal cooling area and heat generated raises the risk of a fire in the battery system [46,47].

Dendrite formation represents a major issue in LIB technology. Li metal has had real appeal as an anode material for LIBs due to its ultrahigh specific capacity of 3860 mAh g<sup>-1</sup>, in addition to its low negative redox potential of -3.04 V in comparison with a standard hydrogen electrode (SHE) [48]. The appearance of lithium dendrite in Li metal batteries is usually associated with abnormal operation conditions like overcharging or charging in low temperatures [49]. Typically, lithium dendrite growth occurs in the presence of

additional lithium ions that accumulate or are deposited on the anode surface, instead of being absorbed or incorporated into the anode [50,51]. As a consequence, lithium ions permeate the separator, giving rise to short circuits, safety issues, and battery failure. In addition, lithium dendrites react with the electrolyte, causing it to decompose through the loss of lithium, thereby diminishing battery capacity [52].

#### 1.1.4. Cathode Materials Applicable in Lithium-Ion Batteries

Among the components in a Li-ion cell, it is the cathodes that restrict energy density and dictate the cost per kilowatt-hour. Modern cathode materials are transition metal oxides, and three classifications of them exist according to their crystal structure: (a) layered  $\text{LiMO}_2$  (M: Ti, V, Cr, Co, Ni), with a two-dimensional layered crystal structure of  $\text{LiCoO}_2$ ; (b) spinel oxides (e.g.,  $\text{LiMn}_2\text{O}_4$ ,  $\text{LiTi}_2\text{O}_4$ ,  $\text{LiNiO}_2$ ) of three-dimensional morphology; and (c) the one-dimensional morphology of polyanion oxides such as  $\text{Li}_2(\text{MoO}_4)_3$ ,  $\text{Li}_2\text{Fe}_2(\text{WO}_4)_3$ , and  $\text{LiFePO}_4$ . In such intercalation cathode materials,  $\text{Li}^+$  is the guest ion that facilitates ion diffusion. Layered and spinel oxides have a close-packed structure with high density, hence they possess sufficient electronic conductivity ( $10^{-1}$ – $10^{-4} \text{ S cm}^{-1}$ ). Although polyanion oxides exhibit low density and poor electronic conductivity, polyanion class cathodes afford high thermal stability and greater safety than layered and spinel oxide cathodes. Figure 2 details the crystal structure of the cathode materials and their voltage profiles [53,54].

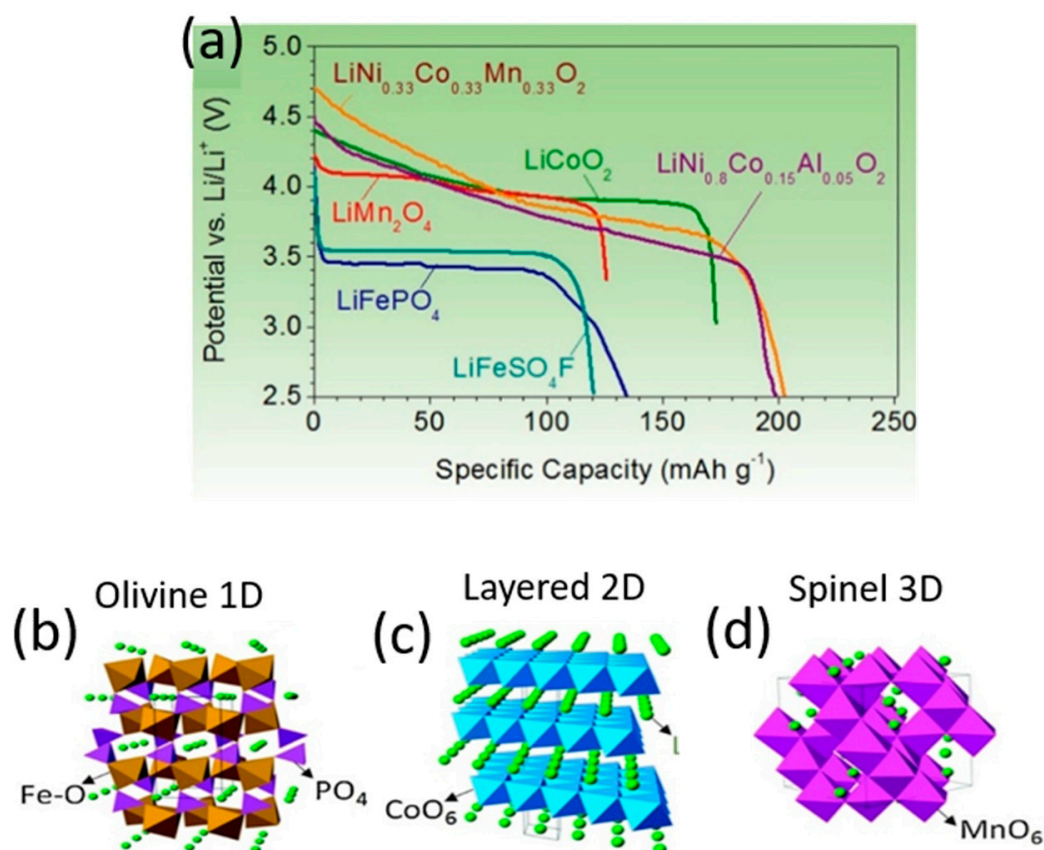


**Figure 2.** Discharge profiles (a) and crystal structures (b–d) of representative intercalation cathodes: olivine  $\text{LiFePO}_4$  (b), layered  $\text{LiCoO}_2$  (c) and spinel  $\text{LiMn}_2\text{O}_4$  (d).

Out of the three classes of oxide cathodes, layered oxides are the preferred option.  $\text{LiNi}_{0.8}\text{Co}_{0.15}\text{Al}_{0.05}\text{O}_2$  and  $\text{LiNi}_{0.33}\text{Co}_{0.33}\text{Mn}_{0.33}\text{O}_2$  demonstrate the highest discharge capacity ( $200 \text{ mAh g}^{-1}$ ) and are commercially applied in Panasonic batteries for Tesla EVs. However, these composite cathode materials demonstrate average discharge voltage decreases during cycling. One way of overcoming this problem is to perform surface stabilization, which minimizes volume changes, cracking, and surface reactivity [54]. It either involves

applying a surface coating by chemical vapor deposition and atomic layer deposition techniques [55], or adding inactive dopant cations into the layered oxide structure. These dopants can substitute Li or transition metal cations; for example, 1–5 mol. % of  $\text{Mg}^{+2}$  cations lead to enhanced cycling stability. Another way pertains to the design of gradient and core-shell cathode particles. Core-shell materials are usually synthesized such that the unstable component is in the core and the thermally stable component constitutes the shell: core (Ni-rich or Li-rich) and shell (Mn-rich) [56]. For instance, the double-shelled material  $\text{Li}[\text{Ni}_{0.8}\text{Co}_{0.1}\text{Mn}_{0.1}]_{2/7}$  core  $[(\text{Ni}_{1/3}, \text{Co}_{1/3}\text{Mn}_{1/3})_{3/14}]$  shell-1  $[\text{Ni}_{0.4}\text{Co}_{0.2}\text{Mn}_{0.4}]_{1/2}\text{O}_2$  shell-2 contributes to the cycling stability of the hybrid structure, resulting in superior electrochemical performance in comparison with a homogeneous cathode with the same overall composition [57]. Different engineering techniques have also been employed to increase the electrochemical performance of a cathode by removing the binder [58] and variously synthesizing carbon-based composite cathodes, e.g., by mixing in CNT and graphene oxide or by applying a coating of conducting polymers, e.g., PANI [59,60].

#### 1.1.5. Anode Materials for Lithium-Ion Batteries

- Lithium-based anodes

In order to achieve a high-energy density and fast charge capability for LIBs, it is necessary to accelerate electrochemical reactions through charge transfer at the interface. Regardless of the fact that Li metal as an anode material has a high theoretical specific capacity (ca  $3860 \text{ mAh g}^{-1}$ ) and the most negative potential ( $-3.040 \text{ V vs. SHE}$ ), it suffers from Li-dendrite formation, poor interfacial contact, notable volume changes and sensitivity of the electrolytes [61]. Various methods exist to regulate Li plating/stripping processes, resulting in formation of “dead Li”, i.e., a protective coating or the design of a composite lithium anode [61]. Creation of a composite lithium anode requires that an additional component is introduced that possesses a similar delithiation potential, and certain reversible storage/release mechanisms of Li ions are in place to facilitate the delithiation mechanism, for example graphene. The cycling performance of a coin cell with a Li metal-graphene anode/LiFSI, DMC, HFE electrolyte/NCM523 cathode maintains 210 cycles with a capacity retention of 80%, in comparison with 110 cycles by a bare Li anode [62]. In practice, though, graphite or graphene is widely applied as an anode material in lithium-ion batteries due to the resultant favorable price-performance ratio [62].

- Graphene-based anodes

The use of graphene as an anode in LIBs makes sense since graphene can accelerate electronic transfer and reduce contact resistance through good contact between the active materials and current collectors, as well as the electrolyte, which reduces polarization. Graphene tends to agglomerate, however, owing to  $\pi$ - $\pi$  interaction and van der Waal forces between layers, potentially hindering its conductivity. Nevertheless, it is possible to take advantage of this property of graphene and modify its structure. In terms of structural form, graphene is available as a material in 1D (fibers), 2D (film and paper), and 3D (hydrogel forms and honeycomb-like structures). Applying such materials as anodes gives rise to superior rates (Table 2) [63].

- Graphite-based anodes

Graphite enables enhanced full cell energy density through its low delithiation potential ( $0.2 \text{ V vs Li/Li}^+$ ) and theoretically high gravimetric capacity ( $372 \text{ mAh g}^{-1}$ ) [64].

Graphite particles are characterized by a flake-like particle morphology with two different surfaces, basal and edge planes (Figure 3) [64]. This 2D-layered structure of graphite causes the anisotropy of surface energy and influences electronic, physicochemical and mechanical properties. Weak van der Waals forces between the graphite layers enable the intercalation of ionic and molecular species across the surfaces. As a result, expansion affects the interlayer distance and re-staking of the graphite layers. A large interlayer separation is favorable for electrode materials as it facilitates lithium-ion intercalation and de-intercalation during charging and discharging. This process ends with the formation of

graphite intercalation compounds (GICs), typically  $\text{LiC}_6$ . GICs possess high reactivity and sensitivity to oxygen and moisture, resulting in rapid material degradation.

**Table 2.** Performance of LIBs with graphene-based anode materials.

Material	Amount of Graphene	Performance
$\text{Li}_4\text{Ti}_5$ /holey-graphene	50 wt. %	98 mAh $\text{cm}^3$ at 17.5 A $\text{g}^{-1}$ ; 84% capacity retention after 1000 cycles at 7 A $\text{g}^{-1}$
$\text{Li}_4\text{Ti}_5$ /graphene	5 wt. %	122 mAh $\text{cm}^3$ at 30°C; 124.5 mA $\text{g}^{-1}$ ; 98% capacity retention after 300 cycles at 20°C
Graphene- $\text{MnO}_2$ -GNRs	68 wt. %	300 mAh $\text{cm}^3$ at 612 mA $\text{g}^{-1}$ after 250 cycles at 0.4 A $\text{g}^{-1}$
$\text{MoS}_2$ -graphene	4.7 wt. %	570 mAh $\text{cm}^3$ at 1A $\text{g}^{-1}$ ; 894.1 mAh $\text{g}^{-1}$ after 100 cycles at 0.1 A $\text{g}^{-1}$
Graphene anchored with $\text{Co}_3\text{O}_4$	24.6 wt. %	484 mAh $\text{g}^{-1}$ at 0.5A $\text{g}^{-1}$ ; 935 mAh $\text{g}^{-1}$ after 30 cycles at 0.1 A $\text{g}^{-1}$ and a specific current of 0.05 A $\text{g}^{-1}$

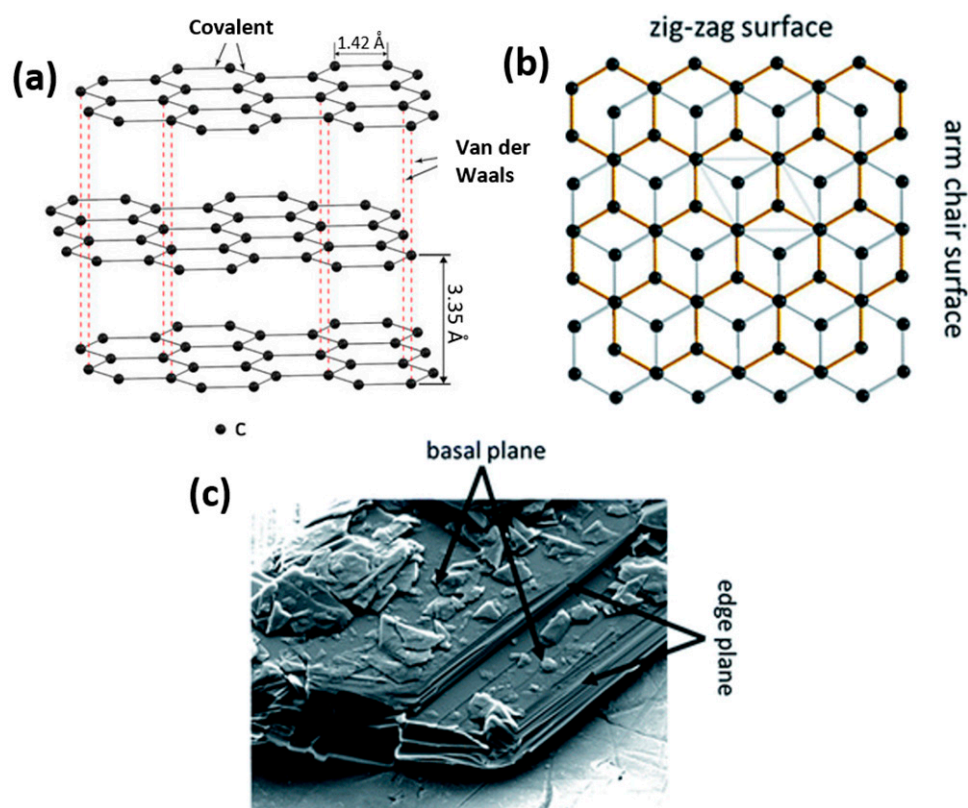


**Figure 3.** Schematic illustration of the layered graphite structure and the resulting presence of basal and edge planes (a) showing the difference between zig-zag and arm chair surfaces (b) and SEM micrograph of the basal and edge planes for a graphite particle (c).

- Ti-based oxides anode materials

This category includes  $\text{TiO}_2$ ,  $\text{Li}_4\text{Ti}_5\text{O}_{12}$ ,  $\text{Li}_2\text{MTi}_3\text{O}_8$ ,  $\text{MLi}_2\text{Ti}_6\text{O}_{14}$  and others, which demonstrate excellent intrinsic safety for their high working potential (1.2–1.7 V vs  $\text{Li}^+/\text{Li}$ ), stable crystal structure during  $\text{Li}^+$  intercalation/de-intercalation, general abundance and low cost, but suffer from poor electronic conductivity ( $10^{-13}$  S  $\text{cm}^{-1}$ ) due to the highest valence state of  $\text{Ti}^{+4}$ , thus restricting their rate capabilities [65,66].

The structural stability, pore size and specific surface area of  $\text{Li}_2\text{ZnTi}_3\text{O}_8$  (LZTO) co-doped with  $\text{Mo}^{6+}$  and  $\text{P}^{5+}$  ions (LZM7TP3O) can be improved by a one-step solid-state technique. When LZM7TP3O is used as the anode in a  $\text{LiNi}_{0.5}\text{Mn}_{1.5}\text{O}_4/\text{LZM}_7\text{TP}_3\text{O}$  full cell, the discharge specific capacity of the full cell reaches  $214.3 \text{ mAh g}^{-1}$  at  $0.5 \text{ C}$  across a voltage range of  $2\text{--}4.55 \text{ V}$  for the 1st cycle [67].

$\text{Li}_4\text{Ti}_5\text{O}_{12}$  is one of the most widely studied complex Ti-based oxides since it is easy to fabricate and boasts a stable voltage plateau, safe performance and long cycling stability; it operates in the potential window of  $1.0\text{--}3.0 \text{ V}$ , delivering a theoretical capacity of  $175 \text{ mAh g}^{-1}$  [68].

The crystal structure of  $\text{Li}_4\text{Ti}_5\text{O}_{12}$  possesses a spinel configuration with an  $\text{Fd}\bar{3}\text{m}$  space group (Figure 4). The 3D structure of  $\text{Li}_4\text{Ti}_5\text{O}_{12}$  secures the presence of the Li-ion transport pathway, which in turn guarantees a stable voltage plateau during lithiation, preventing the formation of lithium dendrites.

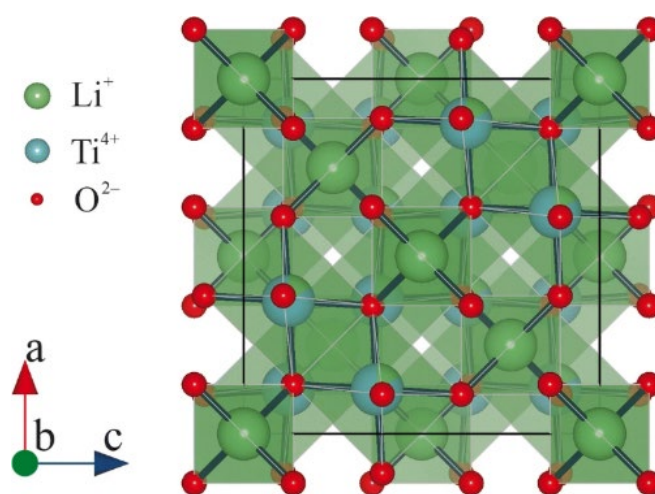


**Figure 4.** Crystal structures of  $\text{Li}_4\text{Ti}_5\text{O}_{12}$ .

In order to enhance the rate capability of  $\text{Li}_4\text{Ti}_5\text{O}_{12}$ , its composites with carbon-based materials have been fabricated by different methods, for example by mixing in CNT or by applying a coating of conducting polymers, e.g., PANI [68,69].

- Silicon-based anode materials

At the outset, graphite-based anodes were successfully adopted to prevent dendrite formation during continuous charge/discharge cycles, and widely deployed in conventional lithium-ion batteries. However, this intercalation type of anode failed to protect the battery from dendrite growth at fast charging rates, while it also has a limited capacity, resulting in poor energy density and restricting the range of EVs. The intercalation speed of lithium-ion into a graphite structure also influences the power of the given cells. Graphite hardly meets the expectations of next generation lithium-ion batteries as a consequence. Silicon was considered as a replacement for graphite anodes, as it boasted much greater lithium storage (approx.  $4000 \text{ mAh g}^{-1}$ ). However, chemical bonds were observed to form during lithium intercalation, giving rise to a new molecular structure, in addition to which the silicon experienced swelling and contraction during a continuous charge-discharge cycle, leading to cracking and pulverization. The SEI layer deformed numerous times when cycling as a consequence, and the related side reaction consumed the lithium in the battery, causing a loss in capacity and increase in cell resistance [70]. Thus, silicon-based LIBs rapidly lose energy storage capability while cycling, and the high cost of silicon limits its applicability in large-scale usage. Numerous strategies have been developed to overcome these defects, notably application of a carbon coating, alloying and construction of porous structures [71,72]. Of the various synthetic methodologies to be researched, the deposition of Si-metal alloys shows promise as a practical means of mass-producing porous

Si microparticles for the reasons of simplicity and low cost [73]. A porous Si anode prepared by dealloying Sr-modified Al–Si alloys is expected to be more effective at mitigating expansion via the introduction of abundant nanoparticles [74]. Compared to graphite and silicon anode-based LIBs, lithium metal may still be the best candidate for several reasons; although the associated drawback of dendrite formation, which diminishes the safety and service life of a lithium metal-based LIB, is likely to restrict its utilization in future high-energy devices.

In addition to the anodes suitable for LIBs mentioned above, an alloying type such as aluminum anodes show potential since they boast a high theoretical capacity (almost  $1\text{Ah g}^{-1}$ ) [75]. Their disadvantage lies in charge transport, as the volume fraction of the surface oxide layer is significant smaller for aluminum particles ( $<10\ \mu\text{m}$ ), having the effect of severely blocking the transport of electrons. Moreover, the poor electrolyte wettability of the surface oxide layer (arising through the low affinity of the solvent molecules for the oxide layer) reduces charge transport. Grafting polar amino groups has been demonstrated as an effective means of improving electrolyte wettability [76].

### 1.2. Challenges Associated with All-Solid-State Batteries

Issues connected with LIB technology in terms of liquid electrolytes and growing demand for energy storage devices has prompted researchers to seek out alternative solutions, ushering in the era of solid-state electrolytes (SSEs) and all-solid-state batteries (ASSBs). SSEs are considered one of the best approaches for solving the lithium dendrite formation in batteries. Replacing volatile, flammable liquid electrolytes with SSEs effectively creates an impenetrable solid barrier to lithium dendrites, allowing the use of a metal lithium anode [77–79]. In an ideal situation, the redox of Li-ion is the only reaction to occur at the anode side, and the lithium stripping and plating are supposed to be homogeneous in ASSBs. It has proven difficult to fabricate such superior ASSBs, though. This is due to the presence of side interfacial reactions that cause instability and the formation of dendrites at the interface of the lithium metal anode, as well as low ionic conductivity and poor physical contact at the cathode interface. This subsequently leads to interfacial degradation, poor cyclic stability, reduced operating speed, and space charge formation layers, among other issues [80].

Interfacial issues that pose challenges in the manufacture and scaling up of ASSBs mainly arise from the instability of SSE. The chemical potential of the highest occupied molecular orbital (HOMO) and lowest unoccupied molecular orbital (LUMO) of the electrolyte determines the stability of the electrolyte. Thus, an interface is thermodynamically stable if the chemical potential of anode and cathode materials is situated between the LUMO and HOMO. Otherwise, an interlayer can appear at both the anode and cathode interface if the chemical potential of the Li metal anode exceeds that of the LUMO, and chemical potential of cathode is less than for the HOMO [81]. Three types of ASSB interface exist: (a) thermodynamically stable (no chemical reactions); (b) non-passivated mixed-conductive interphase; and (c) passivated kinetically stable interphase, created by chemical reactions at the interface of the electrolyte and electrode [82,83]. The mixed-conductive interphase shows high electronic and ionic conductivity, hence decomposition of the electrolyte at this interphase is spontaneous and promotes reduction in the electrolyte [84,85]. However, even in the kinetically stable interphase, reduction in SSE is spontaneous. Nevertheless, the interphase is electronically insulated and the electronic barrier potential decreases across the interphase [86,87]. The chemical reaction at this interface results in a stable solid electrolyte interface with diminished electronic conductivity, further limiting the possibility of additional side reactions. The formation of thermodynamically and kinetically stable interfaces could prove beneficial for the long-term performance of the battery. However, the majority of the reported solid electrolytes are thermodynamically unstable as regards the lithium metal anode, and a kinetically stable, mixed-conductive interface is often observed on the anode side of the solid electrolyte [88,89].

A major problem affecting a solid-state electrolyte is low ionic conductivity. The ion conduction mechanism in SSEs is totally different from that of liquid electrolytes. In the liquid environment, solvated ions involved in the solvation process move easily through the solvent medium [90]. In SSEs, diffusion by the mobile ions through the nonuniform environment is needed to overcome several energy barriers, including motional energy, interactions with the inherent lattice, and electrostatic forces, whereby they greatly influence the ionic conductivity [91,92]. Ion mobility in a crystalline solid also depends on interstitial aspects and interstices, among other things. Crystalline solid materials are composed of coordination polyhedral and spatial arrangements of several mobile species. The polyhedral framework enables numerous vacancies to be distributed within itself. The hopping of the mobile ion through these vacancies contributes to ion transportation. The interface between the cathode and the solid electrolyte is thermodynamically unstable due to unavoidable chemical reactivity at the interface and the restricted electrochemical potential window of the electrolyte [93,94]. At high voltage, the electrolyte tends to decompose, effecting reduction in ionic conductivity. The formation of a space charge layer (SCL) at the solid-solid interface, triggered by a substantial difference in the electrochemical potential of the cathode and the solid-state electrolyte, is another matter for consideration in the rational design of ASSBs. The SCL formed induces a Li-depletion layer, which hinders the transportation of lithium at the interface, especially in sulfide electrolytes [95–98].

#### Solid-State Electrolytes

Studies on SSEs have long been published, and yet huge challenges to their implementation still persist. In order to supersede an organic liquid electrolyte and avoid the safety limits of the existing LIBs, the proposed solid-state electrolytes have to satisfy the following criteria [99–101]:

- Good ionic conductivity and negligible electronic conductivity with a wide working temperature range.
- A chemical potential range between that of the Li metal anode and the corresponding cathode.
- Negligible grain boundary resistance and interface resistance at the electrode-electrolyte interface.
- For high temperature operation, thermal and mechanical properties, e.g., the thermal expansion coefficient, match those of the anode and cathode.
- High chemical stability, in connection with that of the metal anode and high voltage cathode.
- Low cost, environmental safety, easy to scale up and prepare.

SSEs tend to fall under three categories—solid inorganic electrolyte (SIEs), solid polymer electrolyte (SPEs), and solid hybrid electrolytes (SHEs).

- Solid inorganic electrolytes

A solid inorganic electrolyte normally possesses high ionic conductivity, a wide stability window greater than 4.0 V, and excellent thermal stability over 100°C [80]. Several drawbacks are associated with SIEs, however, as follows:

- High fragility.
- Poor contact with the electrode and inferior interfacial charge transport leads to high impedance.
- Dendrite growth and propagation through grain boundaries, especially at lower current densities
- High cost and poor environmental stability.

In the case of SIEs, high ionic conductivity is achieved through the transfer of ions through voids, layered structures, and excess metal ions. The observed ionic conductivity in the SIEs is in the order of  $\text{mS cm}^{-1}$  (see Table 3). High ionic conductivity is achieved in SIEs by reducing the electrostatic force within the material, which enables the transfer of multivalent cations. Reduction in electrostatic force can be accomplished by increasing the

distance between the mobile cation and the nearby anions through the anion framework by ion substitution.

**Table 3.** Ionic conductivity of solid inorganic electrolytes at room temperature.

Solid-State Electrolyte	Composition	Ionic Conductivity S cm <sup>-1</sup>
NASICON-like	Li <sub>1.4</sub> Al <sub>0.4</sub> Ti <sub>1.6</sub> [PO <sub>4</sub> ] <sub>3</sub>	1.12·10 <sup>-3</sup>
LISICON-like	Li <sub>3.25</sub> Ge <sub>0.25</sub> P <sub>0.75</sub> S <sub>4</sub>	10 <sup>-2</sup>
thio-LISICON	Li <sub>9.54</sub> Si <sub>1.74</sub> P <sub>1.74</sub> S <sub>11.7</sub> Cl <sub>0.3</sub>	1.25·10 <sup>-1</sup>
	Li <sub>3.25</sub> Ge <sub>0.25</sub> P <sub>0.75</sub> S <sub>4</sub>	10 <sup>-2</sup> ·10 <sup>-3</sup>
	Li <sub>9.54</sub> Si <sub>1.74</sub> P <sub>1.44</sub> S <sub>11.7</sub> Cl <sub>0.3</sub>	2.5·10 <sup>-2</sup>
Anti-perovskites	Li <sub>3</sub> OX (X = Cl or Br)	>10 <sup>-3</sup>
Garnets	Li <sub>6.55</sub> La <sub>2.5</sub> BaZrTaO <sub>12</sub>	6·10 <sup>-3</sup>
	Li <sub>6.5</sub> La <sub>3</sub> Zr <sub>1.5</sub> Ta <sub>0.5</sub> O <sub>12</sub>	0.75·10 <sup>-3</sup>
	Li <sub>6.25</sub> La <sub>3</sub> Zr <sub>2</sub> Al <sub>0.25</sub> O <sub>12</sub>	0.68·10 <sup>-3</sup>
	Li <sub>6.25</sub> La <sub>3</sub> Zr <sub>2</sub> Ta <sub>0.25</sub> Ga <sub>0.2</sub> O <sub>12</sub>	1.04·10 <sup>-3</sup>
Li <sub>2</sub> S-SiS <sub>2</sub> based	95[0.6Li <sub>2</sub> S0.4SiS <sub>2</sub> ]·5Li <sub>4</sub> SiO <sub>4</sub>	10 <sup>-3</sup>
Li <sub>2</sub> S-P <sub>2</sub> S <sub>5</sub> based	70Li <sub>2</sub> S-30P <sub>2</sub> S <sub>5</sub> glass ceramic	3.2·10 <sup>-3</sup>

- Solid Polymer Electrolytes

Compared to SIEs, SPEs boast numerous advantages, including low cost, ease of fabrication, chemical and thermal stability, the capacity for large-scale manufacture, and mechanical toughness above the glass transition temperature. The strong adhesion of SPEs means they are highly compatible with the electrode material. However, the applicability of SPEs in batteries is also hindered by certain matters. Firstly, the ionic conductivity of most SPEs is limited to between 10<sup>-6</sup> and 10<sup>-5</sup> S cm<sup>-1</sup>, which affects the overall resistance of the battery system [102]. In an ideal case, the lithium migration number is one. If Li<sup>+</sup> migration is too little, then the anions accumulate on the electrode surface and cause concentration polarization. Two methods are adopted to avoid this in SPEs, the first involves grafting anions into the polymer backbone (a common method for preparing single ion conductors), while the other adds an anion acceptor into the polymer matrix to restrict anion movement.

Owing to the merits of SIEs and SPEs, the development of a composite that combines the best of both is of particular interest, and these are referred to as hybrid solid electrolytes or composite electrolytes.

- Solid hybrid electrolytes

As mentioned above, both types of solid electrolyte possess disadvantages. To overcome these issues researchers devised a composite solid-state electrolyte with a combination of polymeric and ceramic structures called a solid hybrid electrolyte (SHE). Through a proper management of composition and an appropriate fabrication process, a resulting polymer-ceramic composite electrolyte could be synthesized with desired and anticipated properties; these include acceptable room temperature Li<sup>+</sup> conductivity, ideal mechanical strength, an extended electrochemical stability window, an improved Li<sup>+</sup> transference number, favorable interfacial contact with electrodes, and dendrite-suppression capability [103]. A polymer matrix is needed to create a SHE, which is filled with an inorganic ceramic filler to increase the ionic conductivity of the composite material. Two groups of such inorganic ceramic fillers exist—passive and active [104]. Passive fillers do not exhibit ionic conductivity themselves, but can promote the ionic properties of polymer matrices. Passive fillers that have been utilized in the studies of Li<sup>+</sup>-ion composite electrolytes include Al<sub>2</sub>O<sub>3</sub> [105], LiAlO<sub>2</sub> [106], TiO<sub>2</sub> [107], SiO<sub>2</sub> [108], Y<sub>2</sub>O<sub>3</sub> [109], ZrO<sub>2</sub> [110], and Mg<sub>2</sub>B<sub>2</sub>O<sub>5</sub> [99].

Active fillers comprise Li-ion conducting materials such as LISICON-type [111], NASICON-type [112], garnet-type [113], perovskite-type [114], sulfide electrolyte [115], and oxy-nitride electrolyte [116].

## 2. Assessment of All-Solid-State Batteries Patents

Innovation in technology requires specific methods of presentation, protection and commercialization are adopted. New technological findings in the field of energy storage technology, such as rechargeable batteries or supercapacitors often appear in the form of a patent proposal. A patent is a form of document that collects together important technological information originating from research that can be later transformed into a commercial product.

There are many aspects related to ASSBs that might be patented, such as materials and electrodes, cells, modules and packaging, reliability, and means of manufacture. Data relating to the patent disclosures investigated below were collected from the European Patent Office. The search process was based on the following keywords: “all-solid-state battery”, “solid-state electrolyte”, ceramic/solid electrolyte” (LIPON,  $\text{Li}_3\text{N}$ , perovskite, garnet, sulfide, LISICON, NASICON-type), “polymer/solid electrolyte” (polysiloxane based, single lithium-ion conductive polymer), “hybrid/solid electrolyte” (ceramic in polymer and vice versa).

Patents and scientific information published pertaining to all-solid-state batteries over the past two decades was analyzed. The various compositions of materials (ceramics, polymers, and mixtures) that shaped the chemical background of solid electrolytes were studied and presented.

An overview of progression in patents over the past two decades, i.e., between the years 2000 and 2020, is displayed in Figure 5, in relation to patents containing the keywords “all-solid-state battery” and “solid-state electrolyte” in the title or abstract. Graphical representation, as shown in the first half of analyzed period (2000–2010), reveals an exceedingly small number of patents related to ASSBs (Figure 5a), with a plateau-like trend and slight incline at the end of the first period (2010). Greater interest was evident for solid-state electrolyte patent applications (Figure 5b), which saw an increase in the second analyzed period (2010–2020), when the number of published patents rose exponentially, peaking at ca 342 patents for ASSBs in 2020 and 67 for SSE in 2019.

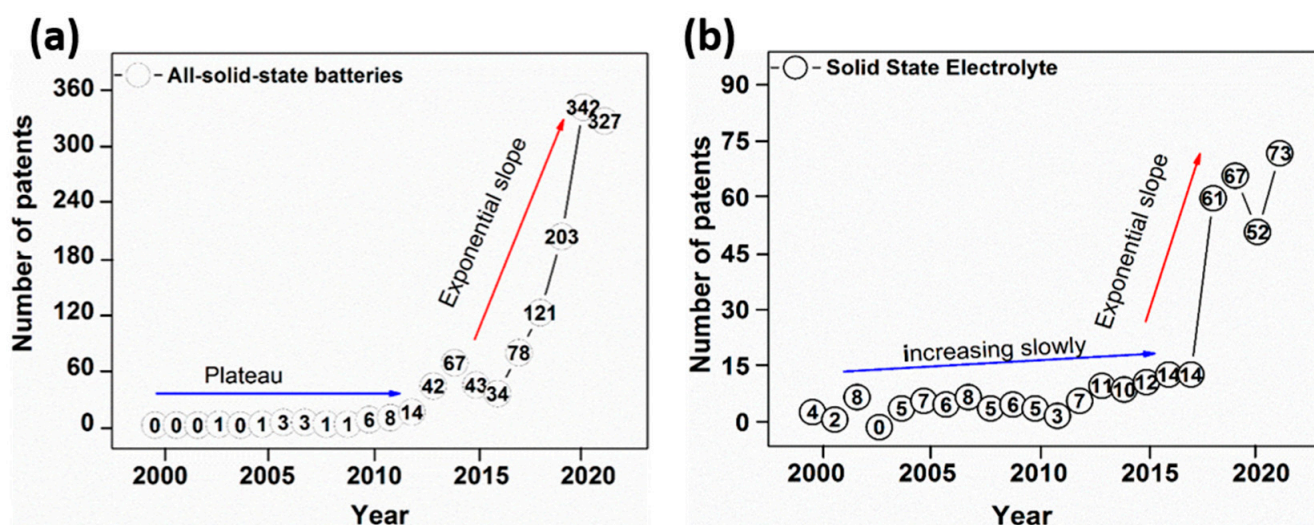


**Figure 5.** Patent applications on all-solid-state batteries (a) and solid-state electrolytes (b) published in the past two decades.

Another interesting aspect concerns the progression of patents published at the end of both examined periods (Figure 6), suggesting that from a total of 26 patents in

2010 (Figure 6a) more than 23% include the key word “all solid-state battery” in the title or abstract, over 53% contain “polymer/solid electrolyte”, in excess of 19% “solid-state electrolyte”, and the remainder of 3.85% ceramic/solid electrolyte “hybrid/solid electrolyte” in 2010 (Figure 6a). The number of patents published rose significantly in 2020 compared to 2010 to 484, out of which 70% related to “all-solid-state batteries”, whereas the rest (13.02%, 10.74%, 3.72%, 1.86%) were about SPE, SSE, SIE, and SHE respectively (Figure 6b).

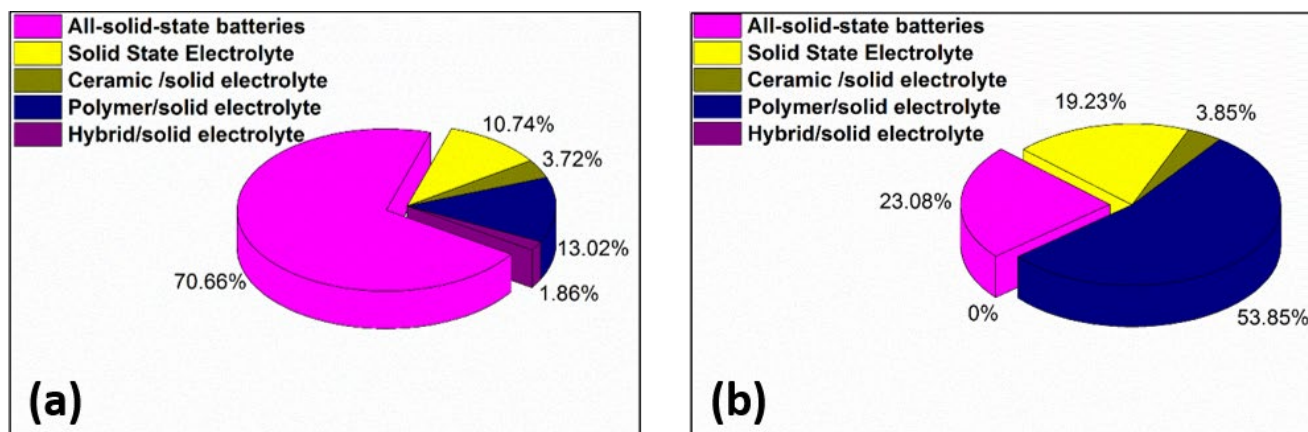


**Figure 6.** Distribution of patent applications on all-solid-state and related compounds for 2010 (a) and 2020 (b).

The investigation continued by taking in some recent patents from 2020 and 2021. The company LG disclosed findings related to ASSBs, and another patent details an electrode assembly and solid electrolyte, wherein the electrode assembly comprises a structure with stacked plate-shaped electrodes, the latter comprising a high heat-generating first electrode and a low heat-generating second one [117]. A method for manufacturing a negative electrode for ASSBs is described in an entry [118]; and the fabrication of a positive electrode for sulfide-based all-solid-state batteries, including preparation of slurry, a coating and a drying process is given [119]. Another innovation presented is a manufacturing technique for creating a positive electrode mixture for all-solid-state batteries, this being a combination of a positive electrode active material and a solid electrolyte in a dry state [120].

### 2.1. Overview of Patents on Solid Inorganic Electrolytes

A visual assessment of patents with the key words “ceramic” or “solid electrolyte” in the title or in abstract is given in Figure 7. A total of 92 patents were registered in the investigated period. Most of them appeared in the second period, specifically after 2018. This trend is expected to continue in the future due to the immense interest shown in ASSBs.

The most widely investigated inorganic materials are  $\text{Li}_{1.4} \text{Al}_{0.4} \text{Ti}_{1.6} [\text{PO}_4]_3$  and NASICON-like,  $\text{Li}_{3.25} \text{Ge}_{0.25} \text{P}_{0.75} \text{S}_4$  (LISICON-like),  $\text{Li}_{6.55} \text{La}_{2.5} \text{BaZrTaO}_{12}$  (Garnet),  $\text{Li}_3 \text{O}_X$  ( $X = \text{Cl}$  or  $\text{Br}$ ) (Perovskite), and  $\text{Li}_2\text{S}-\text{P}_2\text{S}_5$  based (Sulfide) types. They exhibit good ionic conductivity and high electrochemical performance, hence their popularity. Based on the given structure and transformation, a series of patent applications were published. Figure 7b depicts a 3-dimensional representation of patents registered in 2020. From a total number of about 47 patents in that year, more than half related to ceramic/solid electrolytes, followed by sulfides at 17%, and perovskite at 10%. Fewer studies looked at inorganic materials such as LIPON like, constituting just 6% of all the patents.

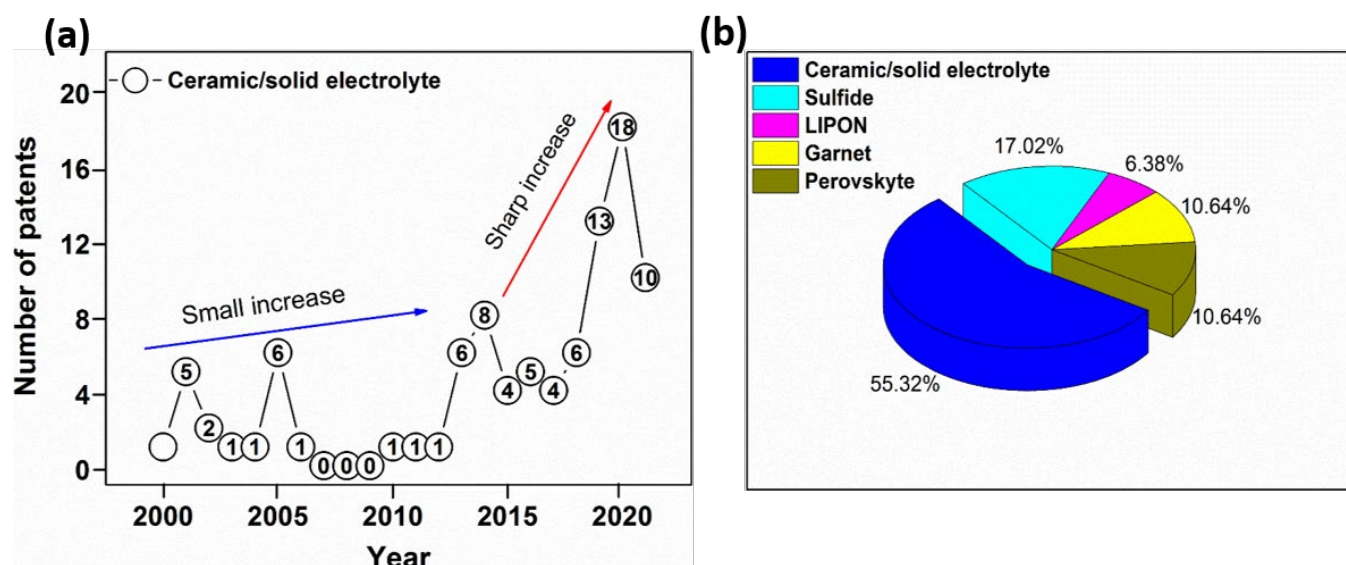


Figure 7. Overview of patents for ceramic/solid electrolytes during 2000–2020.

Other patent statements were assessed, starting with some from the Murata company reporting on a ceramic solid electrolyte of garnet-type supplemented with one or more transition metal elements from the group composed of cobalt (Co), nickel (Ni), manganese (Mn), and iron (Fe) [121–123]. Idemitsu Kosan CO describe an invention of a sulfide solid electrolyte (glass ceramic) boasting high ionic conductivity and improved water resistance, as well as a method for fabricating the sulfide solid electrolyte glass ceramic material [124]. The Yangtze River Delta Institute Of Research have developed a sodium ion solid electrolyte ceramic material with a modified NASICON-type structure; the chemical formula for it is  $\text{Na} < 3 + x + y > \text{Zr} < 2-x > \text{Sc} < x > \text{Si} < 2 + y > \text{P} < 1-y > \text{O} < 12 > (x \leq 0.3, y \leq 0.2)$ , which is stated as having very good conductivity ( $0.7 \times 10^{-3} \text{ S cm}^{-1}$ ) and relatively high sodium ion transmission capability [125].

## 2.2. Solid Polymer Electrolytes

Polymers represent another category of materials which can be utilized to fabricate solid electrolytes due to their stable chemical properties at the electrode/electrolyte interface and action against dendrite growth from the Li metal anode. [126]. For example, polyethylene oxide (PEO) has been widely used over the past two decades as the basis for polymer electrolytes. This composite solid polymer electrolyte is an inorganic fibrous substrate containing PEO, ceramic powder, and a liquid electrolyte with a lithium or sodium salt [127]. Indeed, many inventions integrate polymer materials as a component of a solid-state electrolyte.

A series of patent applications related to different mono/polymeric structures involved in the synthesis of solid-state electrolytes. For example, one invention shows a method for creating a composite SPE with increased strength and productivity through thermocompression bonding of the electrolyte with inorganic fibers [128].

Polymers also prove useful in preparing electrolyte membranes. In this context, a nitrile monomer provides rigidity for an electrolyte membrane with good stability, while a vinyl ester monomer provides flexibility for the electrolyte membrane, so that the former membrane can enhance interfacial contact and ensure mechanical performance [129].

Another invention comprises the preparation of a polymer solid electrolyte by electrospinning thermoplastic polyurethane on a glass fiber cloth, and curing ionic liquid in the spinning thermoplastic polyurethane with the aid of polyurethane acrylate. The resultant electrolyte has the advantages of rapid curing at room temperature, is straightforward to produce, and has good adhesive force and excellent mechanical properties in transverse and normal directions [130]. Patented inventions cover the compositions of polymer solid

electrolytes and methods for their preparation and application. An example of a composite electrolyte has a wide electrochemical window due to the presence of flexible chain segments and rigidity of the benzene ring structure, which ensures plasticity and heightens mechanical strength. The flexible segment of the polymer electrolyte holds a large number of ether-oxygen bonds and can conduct lithium ions, and its rigid structure contains fluorine, trifluoromethyl, sulfamides and other groups with high electron delocalization, thus promoting the dissociation of lithium ions and a rise in ionic conductivity. Furthermore, the polymer electrolyte is a polyanionic single ion conductor and has a relatively high lithium-ion transfer number [131].

This investigation revealed that publications on polymer/solid-state electrolytes are not considered inferior in importance to those on ceramic/solid electrolytes, demonstrating the great interest shown by the scientific and industrial community. A total of 63 patents were published at the end of second investigated period (Figure 8a). A similar trend can be observed with respect to ASSBs, i.e., a continuous increase in patents even after 2020 (22 patents) with 28 new entries (Figure 8b).

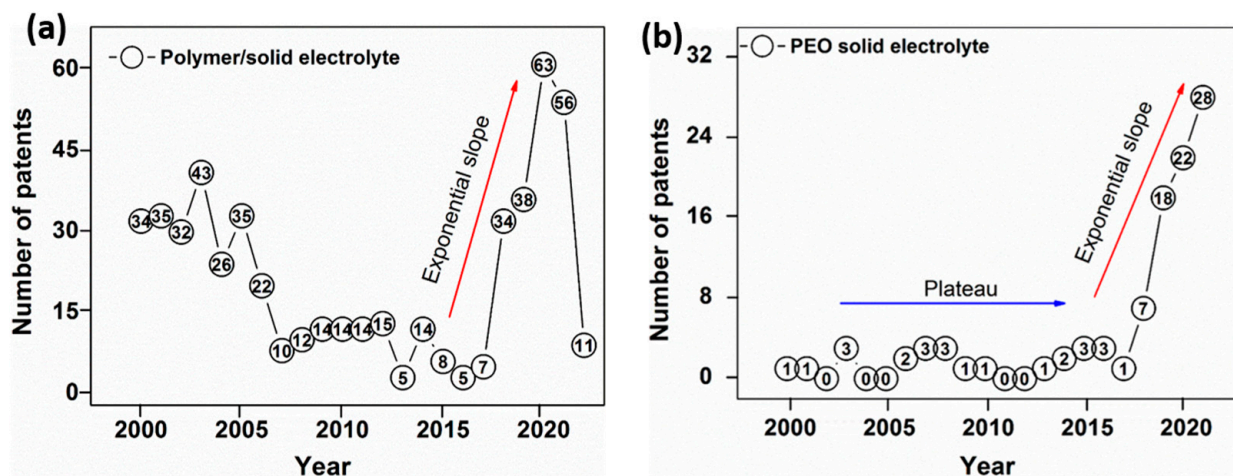


Figure 8. Overview of patent applications on polymer (a) and polyethylene oxide (b) solid electrolytes in 2000–2020.

Figure 9 shows a comparison of the number of patents calculated for both investigated periods. According to the obtained data, the number of patents on solid electrolytes based on PEO increased four-fold, while the total number of published patents rose from 15 in 2010 to 85 in 2020.

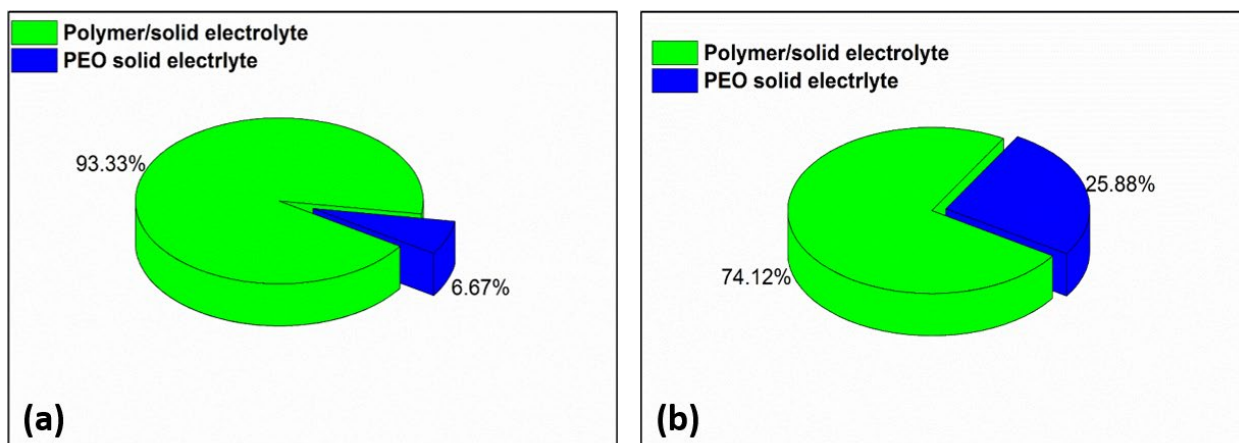
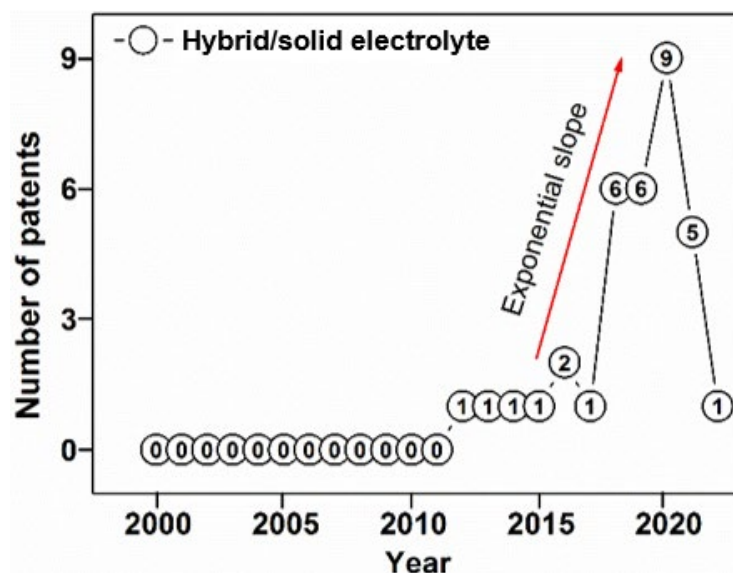


Figure 9. Comparison of distribution of patents on the topics of polymer/solid electrolytes and PEO solid electrolytes in 2010 (a) and 2020 (b).

### 2.3. Overview of Hybrid (Ceramic/Polymer) Solid Electrolytes

To improve the performance of solid electrolytes, scientists propose intercalation of a polymer material with ceramic components to create a hybrid polymer/ceramic electrolyte. As this constitutes a relatively recent advancement, very few patents appeared on the subject in the first half of investigated period (2000–2010) (Figure 10), but more have been published since. It is notable that after 2017 interest in hybrid solid electrolytes technologies increased exponentially, reaching ninth position in relation to patents registered in 2020.



**Figure 10.** Progression of patent applications on hybrid (inorganic-polymeric)/solid electrolytes in 2000–2020.

This review disclosed a method for fabricating an ion-doped, all-solid-state lithium-ion conductive material with lithium ionic conductivity, which included a continuous Taylor flow reactor, and synthesis of a  $\text{LaZrGa}(\text{OH})_x$  metal hydroxide precursor by coprecipitation; the production of free-standing, double-layered or triple-layered organic-inorganic hybrid solid electrolyte membranes is also described, facilitated by applying the all-solid-state lithium-ion conductive material to a polymer material and coating it via a blade coating method [132]. Another patent published in 2021 details a composite solid electrolyte separation membrane that employs an inorganic fiber and a secondary battery with the same fiber, a composite solid electrolyte separation membrane including the inorganic fiber, a sodium oxide-based ceramic material impregnated in the inorganic fiber, and an electrolyte incorporated in the inorganic fiber, into which the sodium oxide-based ceramic material is impregnated [133]. An invention is reported of an all-solid-state secondary lithium battery representing a combination of a sulfide-based solid electrolyte positioned on the positive electrode with an oxide-based solid electrolyte and a second binder, as well as a negative electrode positioned on the solid electrolyte layer incorporating a negative electrode active material [134]. Patents discourse on trends in technological development that could become global products. They usually reflect the market penetration potential of a technology, and aid forecast of the development of a particular technological area. In order to help comprehend and analyze the effectiveness of patent technologies in the market, a separate study of ASSBs companies was conducted, as presented below.

### 3. Global Overview of ASSB-Producing Solid-State Battery Companies

Global demand for ASSBs has grown steadily in recent years due to the fact that solid-state batteries are becoming more readily applied by the automotive, industrial, consumer, and portable electronics industries. Solid-state batteries are safer, more environmentally friendly, and have a higher energy density and longer service life than lithium-ion batteries

with a liquid electrolyte. This makes them an economical and sensible choice in the battery market worldwide. Several international companies have focused on developing and producing solid-state batteries.

At the forefront of innovation in semi solid-state batteries are developers of solid-state batteries for the EV sector, companies, universities, and government agencies. This section provides an overview of companies at the helm of the global solid-state battery market. Based on information gathered from websites, news articles, marketing reports, and scientific journals, a list of such major players was compiled.

Keywords were identified in the Google Ads and Google Trends search tools to define relevant search parameters, as follows: “solid-state electrolyte” (SSE), “all-solid-state battery” (ASSB), “solid-state battery” (SSB), and “solid-state lithium-ion battery”. Using these keywords, leading countries were identified in terms of the number of requests for data for the current year in the Google Trends web app. Then an overview of which countries were actively involved in ASSB development was formed based upon each keyword. Google searches were subsequently carried out, where a query was entered for each key word and country from the compiled list, in order to obtain maximal access to current data on entities participating in ASSB activities. In accordance with corporate web pages, publications on the topic, marketing and scientific reports, and media discussions, a full list of 93 companies and institutions was drawn up with relevance to the creation and development global ASSB market.

The analysis identified 93 companies from various countries, led by the USA, Japan, China, Germany, France, Canada, the UK, and South Korea (Figure 11)

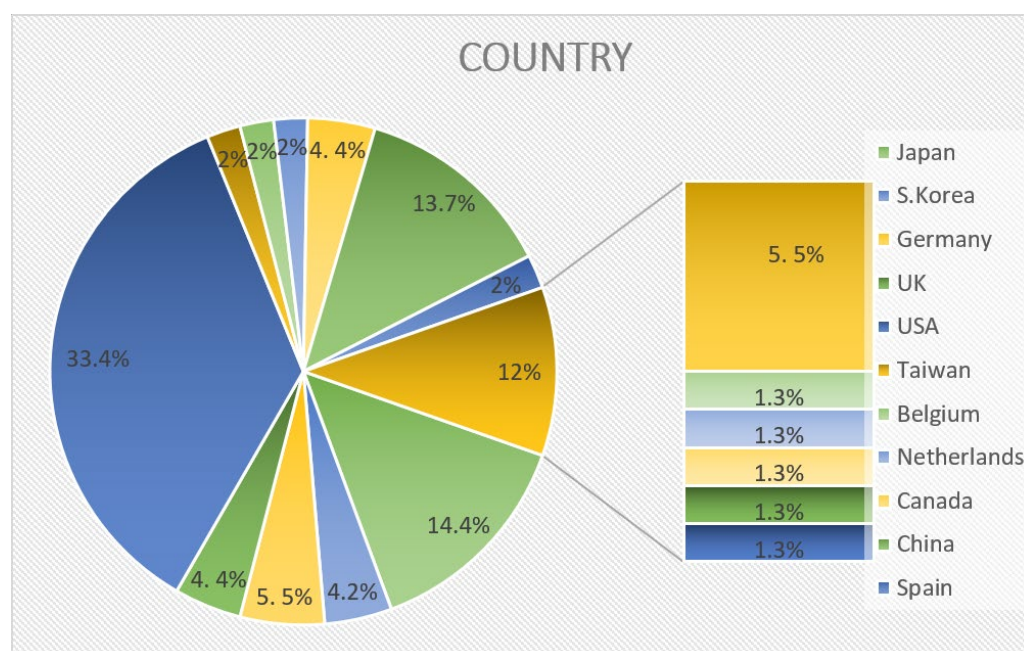


**Figure 11.** Classification based on geographical position of companies participating in ASSB activities.

During the next stage of the analysis, data on the operations of the firms, their research efforts, and the compliance of such technologies with the ASSB concept were studied in detail. Based on the findings, entities were classified according to the following eight criteria:

1. Companies not providing detailed information on ASSBs
2. Suppliers and manufacturers of materials and components for ASSBs
3. Companies applying hybrid technologies
4. Companies cooperating with other firms and investing in the development of ASSBs
5. Companies with their own technology that lack a prototype or device

6. Companies conducting research on the topic that have not openly disclosed any results
7. Companies that have published information on ASSB prototypes
8. Companies with an ASSB product sold commercially

In accordance with the above criteria, 36 companies with ASSB prototypes and devices were selected. These companies were primarily located in developed countries, i.e., the USA, Japan, China, France, Canada, and Great Britain (Figure 12). The automotive sector provides most of the impetus for SSB development, and this is expected to be the main application for SSBs in the medium and long term. Widespread adoption of oxide and sulfide-based SSBs by automotive firms, however, is not anticipated for another five years. Until that time, the emerging market for inorganic SSBs appears to be for consumer goods (e.g., laptops, smartphones, and power tools), as requirements and testing procedures may be less stringent. Vehicle manufacturers are likely to be the primary initial users of oxide SSBs, possibly in parallel with producers of industrial heavy-duty machinery and equipment for harsh environments, as such batteries might prove sufficiently robust. The expense associated with the new technology means that high-end sectors will target SSBs first. Once economies of scale bring about cost reductions, SSBs could become more appealing for further applications, such as truck and stationary storage units. After 2035, SSBs might even find their way into other areas such as passenger aviation. [135]

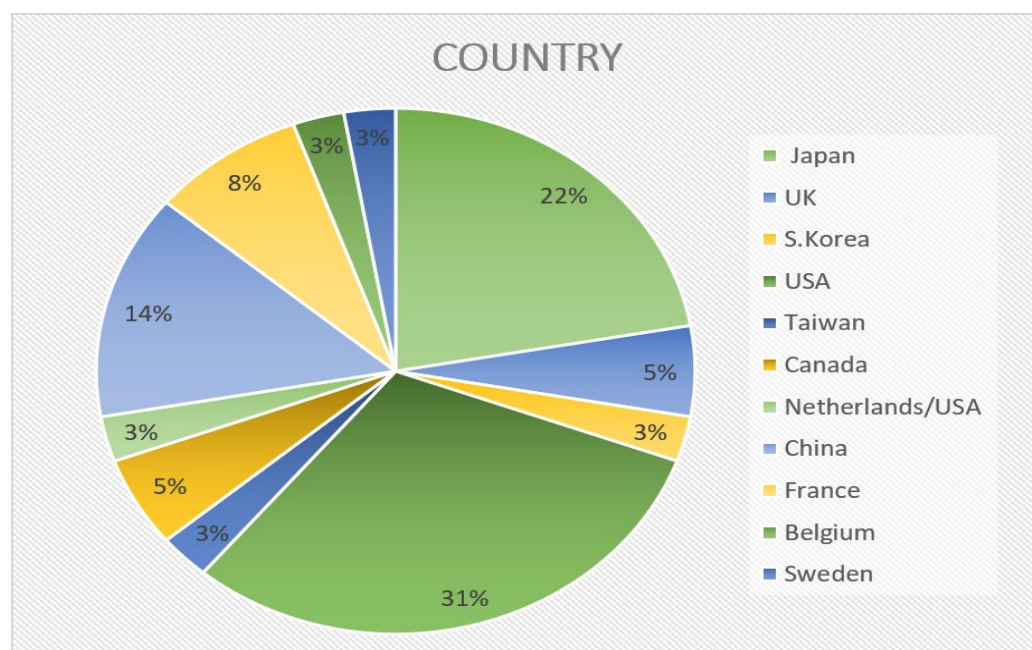


**Figure 12.** Pie chart of companies that claim to have an ASSB prototype or device based on their geographical position.

Various potential business applications exist for ASSBs, as can be seen from the Table 4.

The most important applications for ASSBs are electric vehicles, consumer electronics, and stationary energy storage units (Figure 13). It is expected that more emphasis will be placed on the latter with the aim of ensuring energy independence in Europe in the coming years.

The compositions of materials employed in the fabrication of solid-state electrolytes are illustrated in Figure 14. Inorganic materials were found in almost two-thirds of the companies analyzed. According to the ASSB roadmap prepared by Fraunhofer, the share of ASSBs in the global demand for LIB is currently less than 0.5%. For the sake of comparison, the global battery market is dominated by lead acid batteries and LIBs.

**Table 4.** Industrial sectors applicable for ASSB technology.

Activity	Devices
	EVs, HEVs, EVs with two-wheel battery swapping functionality, electric bicycles, hybrid vehicles
Consumer electronics	Autonomous sensor devices, smart homes (HVAC, security systems, lights); automotive (infotainment systems, sensors); logistics (asset tracking); wearables dedicated to the needs of next generation IoT edge nodes; miniature devices; electronics; standby power supplies; portable devices, the Internet of Things; emergency power protection; watches; autonomous sensors; Real Time Clock (RTC); products with semiconductors; automotive electrical equipment; safety UPS systems
Medicine/Health	Medical devices (biometric monitoring); medical implants; health and fitness applications; other medical applications
Aerospace	Satellites
Industrial	Factory/infrastructure/industrial equipment; rural electrification; hybrid power units for industries manufacturing, and production; 3C consumption industries; patrol inspection security systems; aerial photography and related industries; robotics and AI; IoT devices
Stationary energy storage	Integration of renewables; energy & utilities; localized power sources; power bridging; grid storage; large-scale energy storage
Military	Aviation; marine; defense

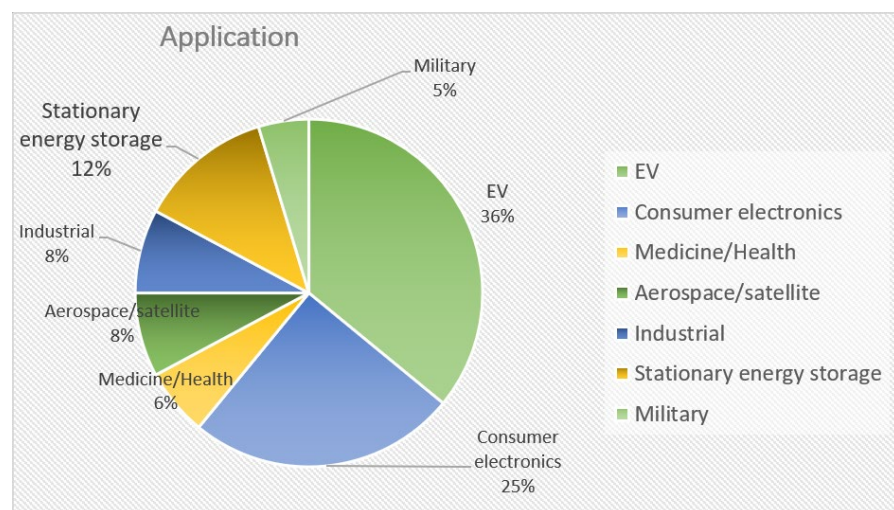


**Figure 13.** Sectors applicable for ASSB use.

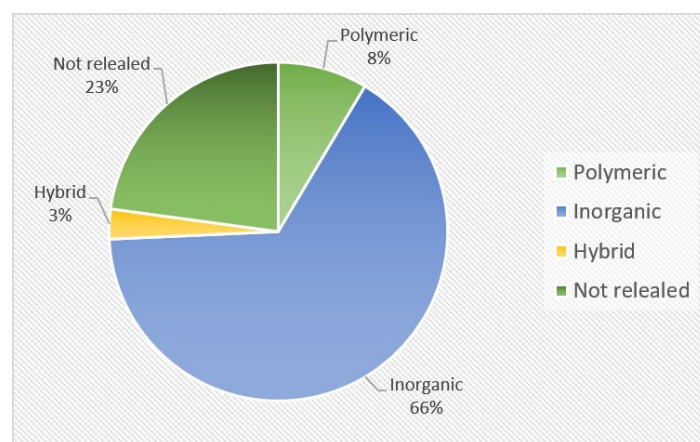


**Figure 14.** Classification of ASSBs based on the material used in the fabrication of SSE.

Even though ASSBs are at a relatively early stage of development and it is difficult to predict the future market, the authors have attempted to make forecasts. In relation to the solid electrolyte (SE), the key component of an ASSB, three material groups stand out as promising candidates—oxide, sulfide, and polymer electrolytes. At the moment, the only solid-state batteries generally available are polymer ASSBs that feature in certain buses.

The current global production capacity of ASSB is estimated to be below 2 GWh, and almost exclusively based on polymer ASSB technology. The Fraunhofer report states that pilot production of polymer-based ASSBs and the initial manufacture of SSB cells with Si anodes and sulfide SE are planned to commence in ca 2025. ASSB pilot production with Li metal anodes and oxide SE is expected to start from 2025 and the sulfide SE-based SSB then 2028.

From an expert ranking, the most promising concepts include ProLogium, Quantum Scape ProLogium (NMC + Gel or Gel + Oxide electrolyte), Solid Power, Samsung-R&D (NMC + sulphide), and Blue Solutions–Bolloré, Hydro Quebec (LFP + polymer electrolyte). The various company announcements are summarized in the Tables contained in the supplementary data [135].

The analysis of companies is complicated by the fact that in an effort to gain a competitive advantage in the global market, many entities have elected for cooperation, leading to a merger of companies or the creation of separate divisions for the research and development of solid-state batteries.

It should be also noted that open data on products are limited, and technical descriptions often lack information, hindering the development of cooperation between companies and research centers.

#### 4. Conclusions, Remarks and Future Perspectives

The transition to clean energy requires the introduction of energy storage devices with excellent electrochemical properties that respect economic, environmental, and social aspects. Analysis of issues associated with liquid electrolytes led scientists in the past to consider solid-state electrolytes, which made it possible to apply a metal lithium anode and design all solid-state batteries. ASSB technology is now a leading contender with respect to energy density and safety.

The purpose of this review article was to analyze the presence of ASSBs in the global market through the evolution of patents, prototypes and devices presented by companies, research centers, and universities.

Research on patents registered in the past two decades showed that references in them to ASSBs saw an exponential increase by 2021. Most of the patents related to solid-state electrolytes, such as solid inorganic electrolytes, where foremost (in terms of the number of patents issued last year) are sulfide, garnet and perovskite types: 196, 42, and 16 respectively. The second most popular were solid polymer electrolytes (SPEs), with over 60 patents, while solid hybrid electrolytes (SHEs) appeared in only 12 patents.

A list of 93 ASSB-associated companies from around the world is provided, based on information available on company websites, social media platforms, and in reports and academic publications. It should be noted that despite the relatively high number of manufacturing companies, most of them do not provide technological information to permit evaluation of the composition and effectiveness of their energy storage devices. Given this fact, for detailed analysis, we selected 35 companies that provided sufficient data on ASSB devices in their product portfolio. According to the results obtained, the USA, Japan, and China are at the forefront of the commercialization of ASSBs, and most of them target EV applications with solid inorganic electrolyte technology.

**Author Contributions:** Conceptualization, C.B.; methodology, C.B. and H.F.; formal analysis, M.V. and A.I.; investigation, C.B., N.E.K., N.J., H.F., M.V. and A.I.; data collection, C.B.; writing—original draft preparation, C.B., N.E.K., N.J. and V.P.; writing—review and editing, C.B., N.E.K. and V.P.; supervision, N.E.K. and P.S.; project administration, V.P.; funding acquisition; All authors have read and agreed to the published version of the manuscript.

**Funding:** This research was funded by the Technology Agency of the Czech Republic, Theta Program, grant number TK03030157.

**Data Availability Statement:** The data presented in this study are available on request from the corresponding author.

**Conflicts of Interest:** The authors declare no conflict of interest.

## References

1. Available online: <https://www.researchandmarkets.com/reports/4396452/lithium-ion-battery-market-size-share-and-trends> (accessed on 15 November 2022).
2. Tarascon, J.M.; Armand, M. Issues and challenges facing rechargeable lithium batteries. *Nature* **2015**, *414*, 359–367. [[CrossRef](#)] [[PubMed](#)]
3. Zhang, X.; Tang, Y.; Zhang, F.; Lee, C.S. A Novel Aluminum–Graphite Dual-Ion Battery. *Adv. Energy Mater.* **2016**, *6*, 1502588. [[CrossRef](#)]
4. Wang, M.; Jiang, C.; Zhang, S.; Song, X.; Tang, Y.; Cheng, H.-M. Reversible calcium alloying enables a practical room-temperature rechargeable calcium-ion battery with a high discharge voltage. *Nat. Chem.* **2018**, *10*, 667–672. [[CrossRef](#)] [[PubMed](#)]
5. Armand, M.; Axmann, P.; Bresser, D.; Copley, M.; Edström, K.; Ekberg, C.; Guyomard, D.; Lestriez, B.; Novák, P.; Petranikova, M.; et al. Lithium-ion batteries—Current state of the art and anticipated developments. *J. Power Sources* **2020**, *479*, 228708. [[CrossRef](#)]
6. Zubi, G.; Dufo-López, R.; Carvalho, M.; Pasaoglu, G. The lithium-ion battery: State of the art and future perspectives. *Renew. Sustain. Energy Rev.* **2018**, *89*, 292–308. [[CrossRef](#)]
7. Chen, Y.; Kang, Y.; Zhao, Y.; Wang, L.; Liu, J.; Li, Y.; Liang, Z.; He, X.; Li, X.; Tavajohi, N.; et al. A review of lithium-ion battery safety concerns: The issues, strategies, and testing standards. *J. Energy Chem.* **2021**, *59*, 83–99. [[CrossRef](#)]
8. Zhang, D.; Tan, C.; Ou, T.; Zhang, S.; Li, L.; Ji, X. Constructing advanced electrode materials for low-temperature lithium-ion batteries: A review. *Energy Rep.* **2022**, *8*, 4525–4534. [[CrossRef](#)]
9. Rodrigues, M.-T.F.; Babu, G.; Gullapalli, H.; Kalaga, K.; Sayed, F.N.; Kato, K.; Joyner, J.; Ajayan, P.M. A materials perspective on Li-Ion batteries at extreme temperatures. *Nat. Energy* **2017**, *2*, 17108. [[CrossRef](#)]
10. Hou, J.; Yang, M.; Wang, D.; Zhang, J. Fundamentals and Challenges of Lithium Ion Batteries at Temperatures between –40 and 60 °C. *Adv. Energy Mater.* **2020**, *10*, 1904152. [[CrossRef](#)]
11. Mizushima, K.; Jones, P.C.; Wiseman, P.J.; Goodenough, J.B.  $\text{Li}_x\text{CoO}_2$  ( $0 < x < 1$ ): A new cathode material for batteries of high energy density. *Mater. Res. Bull.* **1980**, *15*, 783–789. [[CrossRef](#)]
12. Yu, W.; Ou, G.; Qi, L.; Wu, H. Textured  $\text{LiFePO}_4$  Bulk with Enhanced Electrical Conductivity. *J. Am. Ceram. Soc.* **2016**, *99*, 3214–3216. [[CrossRef](#)]
13. Chen, S.-P.; Lv, D.; Chen, J.; Zhang, Y.-H.; Shi, F.-N. Review on Defects and Modification Methods of  $\text{LiFePO}_4$  Cathode Material for Lithium-Ion Batteries. *Energy Fuels* **2022**, *36*, 1232–1251. [[CrossRef](#)]
14. Sharma, N.; Yu, D.H.; Zhu, Y.; Wu, Y.; Peterson, V.K. In operando neutron diffraction study of the temperature and current rate-dependent phase evolution of  $\text{LiFePO}_4$  in a commercial battery. *J. Power Sources* **2017**, *342*, 562–569. [[CrossRef](#)]
15. Liao, L.; Cheng, X.; Ma, Y.; Zuo, P.; Fang, W.; Yin, G.; Gao, Y. Fluoroethylene carbonate as electrolyte additive to improve low temperature performance of  $\text{LiFePO}_4$  electrode. *Electrochim. Acta* **2013**, *87*, 466–472. [[CrossRef](#)]
16. Ma, Q.; Zeng, X.-X.; Yue, J.; Yin, Y.-X.; Zuo, T.-T.; Liang, J.-Y.; Deng, Q.; Wu, X.-W.; Guo, Y.-G. Viscoelastic and Nonflammable Interface Design–Enabled Dendrite-Free and Safe Solid Lithium Metal Batteries. *Adv. Energy Mater.* **2019**, *9*, 1803854. [[CrossRef](#)]
17. Guohua, T. Nonequilibrium Electron-Coupled Lithium Ion Diffusion in  $\text{LiFePO}_4$ : Nonadiabatic Dynamics with Multistate Trajectory Approach. *J. Phys. Chem. C* **2016**, *120*, 6938–6952. [[CrossRef](#)]
18. Tu, W.; Xia, P.; Li, J.; Zeng, L.; Xu, M.; Xing, L.; Zhang, L.; Yu, L.; Fan, W.; Li, W. Terthiophene as electrolyte additive for stabilizing lithium manganese oxide cathode for high energy density lithium-ion batteries. *Electrochim. Acta* **2016**, *208*, 251–259. [[CrossRef](#)]
19. Visco, S.; Katz, B.; Nimon, Y.; De Jonghe, L. Protected Active Metal Electrode and Battery Cell Structures with Non-Aqueous Interlayer Architecture. U.S. Patent US7282295B2, 28 June 2007.
20. Abraham, K.M.; Jiang, J. A Polymer Electrolyte–Based Rechargeable Lithium/Oxygen Battery. *Electrochem. Soc.* **1996**, *143*, 1. [[CrossRef](#)]
21. Laoire, C.Ó.; Mukerjee, S.; Plichta, E.J.; Hendrickson, M.A.; Abraham, K.M. Rechargeable Lithium/TEGDME– $\text{LiPF}_6$ – $\text{O}_2$  Battery. *J. Electrochem. Soc.* **2011**, *158*, A302–A308. [[CrossRef](#)]
22. Herbert, D.; Ulam, Z.U.S. Electric Dry Cells and Storage Batteries. Patent 3043896, 7 October 1962.
23. Bruce, P.G.; Hardwick, L.J.; Abraham, K.M. Lithium-air and lithium-sulfur batteries. *MRS Bull.* **2011**, *36*, 506–512. [[CrossRef](#)]
24. Cai, K.; Wang, T.; Wang, Z.; Wang, J.; Li, L.; Yao, C.; Lang, X. A cocklebur-like sulfur host with the  $\text{TiO}_2$ –VOx heterostructure efficiently implementing one-step adsorption-diffusion-conversion towards long-life Li–S batteries. *Compos. Part B Eng.* **2023**, *249*, 110410. [[CrossRef](#)]
25. Manthiram, A. An Outlook on Lithium Ion Battery Technology. *ACS Cent. Sci.* **2017**, *3*, 1063–1069. [[CrossRef](#)] [[PubMed](#)]

26. Murdock, B.E.; Toghill, K.E.; Tapia-Ruiz, N.A. Perspective on the Sustainability of Cathode Materials used in Lithium-Ion Batteries. *Adv. Energy Mater.* **2021**, *11*, 2102028. [[CrossRef](#)]
27. Wang, C.; Fu, K.; Kammampata, S.P.; McOwen, D.W.; Samson, A.J.; Zhang, L.; Hitz, G.T.; Nolan, A.M.; Wachsman, E.D.; Mo, Y.; et al. Garnet-Type Solid-State Electrolytes: Materials, Interfaces and Batteries. *Chem. Rev.* **2020**, *120*, 4257–4300. [[CrossRef](#)] [[PubMed](#)]
28. Winter, M.; Barnett, B.; Xu, K. Before Li Ion Batteries. *Chem. Rev.* **2018**, *118*, 11433–11456. [[CrossRef](#)]
29. Li, M.; Wang, C.; Chen, Z.; Xu, K.; Lu, J. New Concepts in Electrolytes. *Chem. Rev.* **2020**, *120*, 6783–6819. [[CrossRef](#)]
30. Zu, C.; Yu, H.; Li, H. Enabling the thermal stability of solid electrolyte interphase in Li-ion battery. *InfoMat* **2021**, *3*, 648–661. [[CrossRef](#)]
31. Pinson, M.B.; Bazant, M.Z.J. Theory of SEI Formation in Rechargeable Batteries: Capacity Fade, Accelerated Aging and Lifetime Prediction. *J. Electrochem. Soc.* **2013**, *160*, A243–A250. [[CrossRef](#)]
32. Zhu, W.; Zhou, P.; Ren, D.; Yang, M.; Rui, X.; Jin, C.; Shen, T.; Han, X.; Zheng, Y.; Lu, L.; et al. A mechanistic calendar aging model of lithium-ion battery considering solid electrolyte interface growth. *Int. J. Energy Res.* **2022**, *46*, 15521–15534. [[CrossRef](#)]
33. Hamidah, N.L.; Wang, F.M.; Nugroho, G. The understanding of solid electrolyte interface (SEI) formation and mechanism as the effect of fluoro-o-phenylenedimaleimide (F-MI) additive on lithium-ion battery. *Surf. Interface Anal.* **2019**, *51*, 345–352. [[CrossRef](#)]
34. Feng, X.; Zheng, S.; Ren, D.; He, X.; Wang, L.; Cui, H.; Liu, X.; Jin, C.; Zhang, F.; Xu, C.; et al. Investigating the thermal runaway mechanisms of lithium-ion batteries based on thermal analysis database. *Appl. Energy* **2019**, *246*, 53–64. [[CrossRef](#)]
35. Hou, J.; Lu, L.; Wang, L.; Ohma, A.; Ren, D.; Feng, X.; Li, Y.; Li, Y.; Ootani, I.; Han, X.; et al. Thermal runaway of Lithium-ion batteries employing LiN(SO<sub>2</sub>F)<sub>2</sub>-based concentrated electrolytes. *Nat Commun.* **2020**, *11*, 5100. [[CrossRef](#)]
36. Jia, H.; Xu, W. Nonflammable nonaqueous electrolytes for lithium batteries. *Curr. Opin. Electrochem.* **2021**, *30*, 100781. [[CrossRef](#)]
37. Liu, X.; Ren, D.; Hsu, H.; Feng, X.; Xu, G.-L.; Zhuang, M.; Gao, H.; Lu, L.; Han, X.; Chu, Z.; et al. Thermal runaway of lithium-ion batteries without internal short circuits. *Joule* **2018**, *2*, 2047–2064. [[CrossRef](#)]
38. Ren, D.; Liu, X.; Feng, X.; Lu, L.; Ouyang, M.; Li, J.; He, X. Model-based thermal runaway prediction of lithium-ion batteries from kinetics analysis of cell components. *Appl. Energy* **2018**, *228*, 633–644. [[CrossRef](#)]
39. Swiderska-Mocek, A.; Jakobczyk, P.; Rudnicka, E.; Lewandowski, A. Flammability parameters of lithium-ion battery electrolytes. *J. Mol. Liq.* **2020**, *318*, 113986. [[CrossRef](#)]
40. Kawamura, T.; Kimura, A.; Egashira, M.; Okada, S.; Yamaki, J.-I. Thermal stability of alkyl carbonate mixed-solvent electrolytes for lithium ion cells. *J. Power Sources* **2002**, *104*, 260–264. [[CrossRef](#)]
41. Kawamura, T.; Okada, S.; Yamaki, J.-I. Decomposition reaction of LiPF<sub>6</sub>-based electrolytes for lithium ion cells. *J. Power Sources* **2006**, *156*, 547–554. [[CrossRef](#)]
42. Ping, P.; Wang, Q.; Sun, J.; Xiang, H.; Chen, C. Thermal Stabilities of Some Lithium Salts and Their Electrolyte Solutions with and Without Contact to a LiFePO<sub>4</sub> Electrode. *J. Electrochem. Soc.* **2010**, *157*, A1170. [[CrossRef](#)]
43. Sloop, S.E.; Pugh, J.K.; Wang, S.; Kerr, J.B.; Kinoshita, K. Chemical Reactivity of PF<sub>5</sub> and LiPF<sub>6</sub> in Ethylene Carbonate/Dimethyl Carbonate Solutions. *Electrochem. Solid-State Lett.* **2001**, *4*, A42. [[CrossRef](#)]
44. Feng, X.; Ouyang, M.; Liu, X.; Lu, L.; Xia, Y.; Hei, X. Thermal runaway mechanism of lithium ion battery for electric vehicles: A review. *Energy Storage Mater.* **2018**, *10*, 246–267. [[CrossRef](#)]
45. Tian, X.; Yi, Y.; Fang, B.; Yang, P.; Wang, T.; Liu, P.; Qu, L.; Li, M.; Zhang, S. Design Strategies of Safe Electrolytes for Preventing Thermal Runaway in Lithium Ion Batteries. *Chem. Mater.* **2020**, *32*, 9821–9848. [[CrossRef](#)]
46. Wang, Z.; Zhu, L.; Liu, J.; Wang, J.; Yan, W. Gas Sensing Technology for the Detection and Early Warning of Battery Thermal Runaway: A Review. *Energy Fuels* **2022**, *36*, 6038–6057. [[CrossRef](#)]
47. Zhang, Q.; Zhang, X.; Yuan, H.; Huang, J. Thermally Stable and Nonflammable Electrolytes for Lithium Metal Batteries: Progress and Perspectives. *Small Sci.* **2021**, *1*, 2100058. [[CrossRef](#)]
48. Liu, H.; Cheng, X.-B.; Jin, Z.; Zhang, R.; Wang, G.; Chen, L.-Q.; Liu, Q.-B.; Huang, J.-Q.; Zhang, Q. Recent advances in understanding dendrite growth on alkali metal anodes. *Energy. Chem.* **2019**, *1*, 100003. [[CrossRef](#)]
49. Kamesui, G.; Nishikawa, K.; Matsushima, H.; Ueda, M. In Situ Observation of Cu<sup>2+</sup> Concentration Profile during Cu Dissolution in Magnetic Field. *J. Electrochem. Soc.* **2021**, *168*, 031507. [[CrossRef](#)]
50. Zhang, X.; Wang, A.; Liu, X.; Luo, J. Dendrites in Lithium Metal Anodes: Suppression, Regulation, and Elimination. *Acc. Chem. Res.* **2019**, *52*, 3223–3232. [[CrossRef](#)]
51. Lee, B.; Paek, E.; Mitlin, D.; Lee, S.W. Sodium Metal Anodes: Emerging Solutions to Dendrite Growth. *Chem. Rev.* **2019**, *119*, 5416–5460. [[CrossRef](#)]
52. Roth, E.P.; Orendorff, C.J. How Electrolytes Influence Battery Safety. *Electrochem. Soc. Interface* **2012**, *21*, 45. [[CrossRef](#)]
53. Manthiram, A. A reflection on lithium-ion battery cathode chemistry. *Nat. Commun.* **2020**, *11*, 1550. [[CrossRef](#)]
54. Booth, S.G.; Nedoma, A.J.; Anthonisamy, N.N.; Baker, P.J.; Boston, R.; Bronstein, H.; Clarke, S.J.; Cussen, E.J.; Daramalla, V.; De Volder, M.; et al. Perspectives for next generation lithium-ion battery cathode materials. *APL Mater.* **2021**, *9*, 109201. [[CrossRef](#)]
55. Zhou, F.; Zhao, X.; van Bommel, A.; Rowe, A.W.; Dahn, J.R. Coprecipitation Synthesis of Ni<sub>x</sub>Mn<sub>1-x</sub>(OH)<sub>2</sub> Mixed Hydroxides. *Chem. Mater. A* **2010**, *22*, 1015–1021. [[CrossRef](#)]
56. Sun, Y.-K.; Myung, S.-T.; Kim, M.-H.; Prakash, J.; Amine, K. Synthesis and Characterization of Ni[(Ni<sub>0.8</sub>Co<sub>0.1</sub>Mn<sub>0.1</sub>)<sub>0.8</sub>(Ni<sub>0.5</sub>Mn<sub>0.5</sub>)<sub>0.2</sub>]O<sub>2</sub> with the Microscale Core–Shell Structure as the Positive Electrode Material for Lithium Batteries. *Am. Chem. Soc.* **2005**, *127*, 13411–13418. [[CrossRef](#)]

57. Hou, P.; Guo, J.; Song, D.; Zhang, J.; Zhou, E.; Zhang, L. A Novel Double-shelled  $\text{LiNi}_{0.5}\text{Co}_{0.2}\text{Mn}_{0.3}\text{O}_2$  Cathode Material for Li-ion Batteries. *Chem. Lett.* **2012**, *41*, 1712–1714. [CrossRef]
58. Bubulinca, C.; Sapurina, I.; Kazantseva, N.E.; Vilčáková, J.; Cheng, Q.; Saha, P. Fabrication of a flexible binder-free lithium manganese oxide cathode for secondary Li—Ion batteries. *J. Phys. Chem. Solids* **2020**, *137*, 109222. [CrossRef]
59. Bubulinca, C.; Sapurina, I.; Kazantseva, N.E.; Pechancova, V.; Saha, P. A Self-Standing Binder-Free Biomimetic Cathode Based on LMO/CNT Enhanced with Graphene and PANI for Aqueous Rechargeable Batteries. *Int. J. Mol. Sci.* **2022**, *23*, 1457. [CrossRef]
60. Sapurina, I.; Bubulinca, C.; Trchová, M.; Prokeš, J.; Stejskal, J. Solid manganese dioxide as heterogeneous oxidant of aniline in the preparation of conducting polyaniline or polyaniline/manganese dioxide composites. *Colloids Surf. A Physicochem. Eng. Asp.* **2022**, *638*, 128298. [CrossRef]
61. Shi, P.; Hou, L.-P.; Jin, C.-B.; Xiao, Y.; Yao, Y.-X.; Xie, J.; Li, B.-Q.; Zhang, X.-Q.; Zhang, Q. A successive conversion-deintercalation delithiation mechanism for practical composite lithium anodes. *J. Am. Chem. Soc.* **2022**, *144*, 212–218. [CrossRef]
62. Nitta, N.; Wu, F.; Lee, J.T.; Yushin, G. Li-ion battery materials: Present and future. *Mater. Today* **2015**, *18*, 252–264. [CrossRef]
63. Sun, D.; Tan, Z.; Tian, X.; Ke, F.; Wu, Y.; Zhang, J. Graphene: A promising candidate for charge regulation in high-performance lithium-ion batteries. *Nano Res.* **2021**, *14*, 4370–4385. [CrossRef]
64. Asenbauer, J.; Eisenmann, T.; Kuenzel, M.; Kazzazi, A.; Chen, Z.; Bresser, D. The success story of graphite as a lithium-ion anode material—fundamentals, remaining challenges, and recent developments including silicon (oxide) composites. *Sustain. Energy Fuels* **2020**, *4*, 5387–5416. [CrossRef]
65. Lou, S.; Zhao, Y.; Wang, J.; Yin, G.; Du, C.; Sun, X. Ti-Based Oxide Anode Materials for Advanced Electrochemical Energy Storage: Lithium/Sodium Ion Batteries and Hybrid Pseudocapacitors. *Small* **2019**, *15*, 1904740. [CrossRef] [PubMed]
66. Li, R.; Lin, C.; Wang, N.; Luo, L.; Chen, Y.; Li, J.; Guo, Z. Advanced composites of complex Ti-based oxides as anode materials for lithium-ion batteries. *Adv. Compos. Hyb. Mat.* **2018**, *3*, 440–459. [CrossRef]
67. Zhang, Z.; Feng, L.; Liu, H.; Wang, L.; Wang, S.; Tang, Z.  $\text{Mo}^{6+}$ - $\text{P}^{5+}$  co-doped  $\text{Li}_2\text{ZnTi}_3\text{O}_8$  anode for Li-storage in a wide temperature range and applications in  $\text{LiNi}_{0.5}\text{Mn}_{1.5}\text{O}_4/\text{Li}_2\text{ZnTi}_3\text{O}_8$  full cells. *Inorg. Chem. Fron.* **2021**, *9*, 35–43. [CrossRef]
68. Sun, L.; Kong, W.; Wu, H.; Wu, Y.; Wang, D.; Zhao, F.; Jiang, K.; Li, Q.; Wang, J.; Fan, S. Mesoporous  $\text{Li}_4\text{Ti}_5\text{O}_{12}$  nanoclusters anchored on super-aligned carbon nanotubes as high-performance electrodes for lithium ion batteries. *Nanoscale* **2016**, *8*, 617–625. [CrossRef]
69. Huang, Z.; Luo, P. Insight into the effects of conductive PANI layer on  $\text{Li}_4\text{Ti}_5\text{O}_{12}$  nanofibers anode for lithium-ion batteries. *Solid State Ion.* **2017**, *311*, 52–57. [CrossRef]
70. Bresser, D.; Paillard, E.; Passerini, S. *Advances in Batteries for Medium and Large-Scale Energy Storage*; Elsevier: Amsterdam, The Netherlands, 2014; pp. 125–211.
71. He, W.; Tian, H.J.; Xin, F.X.; Han, W.Q. Scalable fabrication of micro-sized bulk porous Si from Fe–Si alloy as a high-performance anode for lithium-ion batteries. *J. Mater. Chem. A* **2015**, *3*, 17956–17962. [CrossRef]
72. Mados, E.; Harpak, N.; Levi, G.; Patolsky, E.; Peled, E.; Golodniitsky, D. Synthesis and electrochemical performance of silicon-nanowire alloy anodes. *RSC Adv.* **2021**, *11*, 26586–28593. [CrossRef]
73. Wang, F.; Sun, L.; Zi, W.W.; Zhao, B.X.; Du, H.B. Solution Synthesis of Porous Silicon Particles as an Anode Material for Lithium Ion Batteries. *Chem. Eur. J.* **2019**, *25*, 9071–9077. [CrossRef]
74. Liu, Q.; Liu, M.W.; Xu, C.; Xiao, W.L.; Yamagata, H.; Xie, S.H. Effects of Sr, Ce and P on the microstructure and mechanical properties of rapidly solidified Al-7Si alloys. *Mater. Charact.* **2018**, *140*, 290. [CrossRef]
75. Wang, M.; Zhang, F.; Lee, C.-S.; Tang, Y.B. Low-Cost Metallic Anode Materials for High Performance Rechargeable Batteries. *Adv. Energy Mater.* **2017**, *7*, 1700536. [CrossRef]
76. Jiang, C.; Zheng, Y.; Wang, D.; Zheng, Y.; Xie, C.; Shi, L.; Liu, Z.; Tang, Y. Unusual Size Effect in Ion and Charge Transport in Micron-sized Particulate Aluminum Anodes of Lithium-ion Batteries. *Angew. Chem. Int. Ed.* **2022**, *61*, e202208370. [CrossRef]
77. Goodenough, B.J. How we made the Li-ion rechargeable battery. *Nat. Electron.* **2018**, *1*, 204. [CrossRef]
78. 2022. Available online: <https://www.quantumscape.com/resources/blog/the-advantages-of-lithium-metal-anodes/> (accessed on 25 July 2022).
79. Tong, Z.; Wang, S.-B.; Liao, Y.-K.; Hu, S.-F.; Liu, R.-S. Interface Between Solid-State Electrolytes and Li-Metal Anodes: Issues, Materials, and Processing Routes. *ACS Appl. Mater. Interfaces* **2020**, *12*, 47181–47196. [CrossRef]
80. Chung, H.; Kang, B. Mechanical and Thermal Failure Induced by Contact between a  $\text{Li}_{1.5}\text{Al}_{0.5}\text{Ge}_{1.5}(\text{PO}_4)_3$  Solid Electrolyte and Li Metal in an All Solid-State Li Cell. *Chem. Mat.* **2017**, *29*, 8611–8619. [CrossRef]
81. Lou, S.; Zhang, F.; Fu, C.; Chen, M.; Ma, Y.; Yin, G.; Wang, J. Interface Issues and Challenges in All-Solid-State Batteries: Lithium, Sodium, and Beyond. *Adv. Mater.* **2021**, *33*, 2000721. [CrossRef]
82. Wu, X.; Jiulin, W.; Fei, D.; Xilin, C.; Nasybulin, E.; Zhang, Y.; Zhang, J.-G. Lithium metal anodes for rechargeable batteries. *Energy Environ. Sci.* **2014**, *7*, 513–537. [CrossRef]
83. Wenzel, S.; Leichtweiss, T.; Krüger, D.; Sann, J.; Janek, J. Interphase formation on lithium solid electrolytes—An in-situ approach to study interfacial reactions by photoelectron spectroscopy. *Solid State Ion.* **2015**, *278*, 98–105. [CrossRef]
84. Wan, J.; Yan, H.-J.; Wen, R.; Wan, L.-J. In Situ Visualization of Electrochemical Processes in Solid-State Lithium Batteries. *ACS Energy Lett.* **2022**, *7*, 2988–3002. [CrossRef]
85. Han, F.; Zhu, Y.; He, X.; Mo, Y.; Wang, C. Electrochemical Stability of  $\text{Li}_{10}\text{GeP}_2\text{S}_{12}$  and  $\text{Li}_7\text{La}_3\text{Zr}_2\text{O}_{12}$  Solid Electrolytes. *Adv. Energy Mater.* **2016**, *6*, 1501590. [CrossRef]

86. Cheng, X.-B.; Zhang, R.; Zhao, C.-Z.; Zhang, Q. Toward Safe Lithium Metal Anode in Rechargeable Batteries: A Review. *Chem. Rev.* **2017**, *117*, 10403–10473. [[CrossRef](#)] [[PubMed](#)]
87. Rettenwander, D.; Wagner, R.; Reyer, A.; Bonta, M.; Cheng, L.; Doeff, M.M.; Limbeck, A.; Wilkening, M.; Amthauer, G. Interface Instability of Fe-Stabilized  $\text{Li}_7\text{La}_3\text{Zr}_2\text{O}_{12}$  versus Li Metal. *J. Phys. Chem. C* **2018**, *122*, 3780–3785. [[CrossRef](#)] [[PubMed](#)]
88. Yang, K.; Leu, I.; Fung, K.; Hon, M.; Hsu, M.; Hsiao, Y.; Wang, M. Mechanism of the interfacial reaction between cation-deficient  $\text{La}_{0.56}\text{Li}_{0.33}\text{TiO}_3$  and metallic lithium at room temperature. *J. Mater. Res.* **2006**, *23*, 1813–1825. [[CrossRef](#)]
89. Gao, Z.; Sun, H.; Fu, L.; Ye, F.; Zhang, Y.; Luo, W.; Huang, Y. Promises, Challenges, and Recent Progress of Inorganic Solid-State Electrolytes for All-Solid-State Lithium Batteries. *Adv. Mater.* **2018**, *30*, 1705702. [[CrossRef](#)] [[PubMed](#)]
90. Bachman, J.C.; Muy, S.; Grimaud, A.; Chang, H.-H.; Pour, N.; Lux, S.F.; Paschos, O.; Maglia, F.; Lupart, S.; Lamp, P.; et al. Inorganic Solid-State Electrolytes for Lithium Batteries: Mechanisms and Properties Governing Ion Conduction. *Chem. Rev.* **2016**, *116*, 140–162. [[CrossRef](#)]
91. Goodenough, J.B. Oxide-Ion Electrolytes. *Annu. Rev. Mater. Res.* **2003**, *33*, 91–128. [[CrossRef](#)]
92. Paul, P.P.; Chen, B.-R.; Langevin, A.S.; Dufek, J.E.; Weker Nelson, J.; Ko, S.J. Interfaces in all solid-state Li-metal batteries: A review on instabilities, stabilization strategies, and scalability. *Energy Storage Mater.* **2022**, *45*, 969–1001. [[CrossRef](#)]
93. Sheng, O.; Jin, C.; Ding, X.; Liu, T.; Wan, Y.; Liu, Y.; Nai, J.; Wang, Y.; Liu, C.; Tao, X. A Decade of Progress on Solid-State Electrolytes for Secondary Batteries: Advances and Contributions. *Adv. Funct. Mater.* **2021**, *31*, 2100891. [[CrossRef](#)]
94. Takada, K. Interfacial Nano architectonics for Solid-State Lithium Batteries. *Langmuir* **2013**, *29*, 7538–7541. [[CrossRef](#)]
95. Gittleson, S.F.; El Gabaly, F. Non-Faradaic  $\text{Li}^+$  Migration and Chemical Coordination across Solid-State Battery Interfaces. *Nano Lett.* **2017**, *17*, 6974–6982. [[CrossRef](#)]
96. Gao, B.; Jalem, R.; Ma, Y.; Tateyama, Y.  $\text{Li}^+$  Transport Mechanism at the Heterogeneous Cathode/Solid Electrolyte Interface in an All-Solid-State Battery via the First-Principles Structure Prediction Scheme. *Chem. Mat.* **2020**, *32*, 85–96. [[CrossRef](#)]
97. Kammampata, S.P.; Thangadurai, V. Cruising in ceramics—Discovering new structures for all-solid-state batteries—Fundamentals, materials, and performances. *Ionics* **2018**, *24*, 639–660. [[CrossRef](#)]
98. Thangadurai, V.; Chen, B. Solid Li- and Na-Ion Electrolytes for Next Generation Rechargeable Batteries. *Chem. Mat.* **2022**, *34*, 6637–6658. [[CrossRef](#)]
99. Thangadurai, V.; Weppner, W. Recent progress in solid oxide and lithium ion conducting electrolytes research. *Ionics* **2006**, *12*, 81–92. [[CrossRef](#)]
100. Thangadurai, V.; Narayanan, S.; Pinzaru, D. Garnet-type solid-state fast Li ion conductors for Li batteries: Critical review. *Chem. Soc. Rev.* **2014**, *43*, 4714–4727. [[CrossRef](#)]
101. Manthiram, A.; Yu, X.W.; Wang, S.F. Lithium battery chemistries enabled by solid-state electrolytes. *Nat. Rev. Mater.* **2017**, *2*, 16103. [[CrossRef](#)]
102. Yao, P.H.; Yu, H.B.; Ding, Z.Y.; Liu, P.C.; Lu, J.; Lavorgna, M.; Wu, J.W.; Liu, X.J. Review on polymer-based composite electrolytes for lithium batteries. *Front. Chem.* **2019**, *7*, 00522. [[CrossRef](#)]
103. An, Y.; Han, X.; Liu, Y.; Azhar, A.; Na, J.; Nanjundan, A.K.; Wang, S.; Yu, J.; Yamauchi, Y. Progress in Solid Polymer Electrolytes for Lithium-Ion Batteries and Beyond. *Small* **2022**, *18*, 2103617. [[CrossRef](#)]
104. Stephan, A.M.; Nahm, K.S. Review on composite polymer electrolytes for lithium batteries. *Polymer* **2006**, *47*, 5952–5964. [[CrossRef](#)]
105. Blake, A.J.; Kohlmeyer, R.R.; Hardin, J.O.; Carmona, E.A.; Maruyama, B.; Berrigan, J.D.; Huang, H.; Durstock, M.F. 3D Printable ceramic-polymer electrolytes for flexible high-performance Li-ion batteries with enhanced thermal stability. *Adv. Energy Mater.* **2017**, *7*, 1602920. [[CrossRef](#)]
106. Mastragostino, M.; Soavi, F.; Zanelli, A. Improved composite materials for rechargeable lithium metal polymer batteries. *J. Power Sources* **1999**, *81*, 729–733. [[CrossRef](#)]
107. Kumar, B.; Scanlon, L.G. Polymer-ceramic composite electrolytes: Conductivity and thermal history effects. *Solid State Ion.* **1999**, *124*, 239–254. [[CrossRef](#)]
108. Zhou, D.; Liu, R.L.; He, Y.B.; Li, F.Y.; Liu, M.; Li, B.H.; Yang, Q.H.; Cai, Q.; Kang, F.Y.  $\text{SiO}_2$  Hollow nanosphere-based composite solid electrolyte for lithium metal batteries to suppress lithium dendrite growth and enhance cycle life. *Adv. Energy Mater.* **2016**, *6*, 1502214. [[CrossRef](#)]
109. Liu, W.; Lin, D.C.; Sun, J.; Zhou, G.M.; Cui, Y. Improved lithium ionic conductivity in composite polymer electrolytes with oxide-ion conducting nanowires. *ACS Nano* **2016**, *10*, 11407–11413. [[CrossRef](#)]
110. Solarajan, A.K.; Murugadoss, V.; Angaiyah, S. Dimensional stability and electrochemical behavior of  $\text{ZrO}_2$  incorporated electrospun PVDF-HFP based nanocomposite polymer membrane electrolyte for Li-ion capacitors. *Sci. Rep.* **2017**, *7*, 45390. [[CrossRef](#)]
111. Sheng, O.W.; Jin, C.B.; Luo, J.M.; Yuan, H.D.; Huang, H.; Gan, Y.P.; Zhang, J.; Xia, Y.; Liang, C.; Zhang, W.K.; et al.  $\text{Mg}_2\text{B}_2\text{O}_5$  Nanowire enabled multifunctional solid-state electrolytes with high ionic conductivity, excellent mechanical properties, and flame-retardant performance. *Nano Lett.* **2018**, *18*, 3104–3112. [[CrossRef](#)]
112. Aono, H.; Sugimoto, E.; Sadaoka, Y.; Imanaka, N.; Adachi, G. Ionic-conductivity and sinterability of lithium titanium phosphate system. *Solid State Ion.* **1990**, *40–41*, 38–42. [[CrossRef](#)]
113. Kasper, H.M. A new series of rare Earth garnets  $\text{LiN}_{3+3}\text{M}_2\text{Li}_3\text{O}_{12}$  ( $\text{M} = \text{Te, W}$ ). *Inorg. Chem.* **1969**, *8*, 1000–1002. [[CrossRef](#)]
114. Inaguma, Y.; Chen, L.Q.; Itoh, M.; Nakamura, T.; Uchida, T.; Ikuta, H.; Wakihara, M. High ionic-conductivity in lithium lanthanum titanate. *Solid State Commun.* **1993**, *86*, 689–693. [[CrossRef](#)]

115. Kennedy, J.H.; Sahami, S.; Shea, S.W.; Zhang, Z.M. Preparation and conductivity measurements of  $\text{SiS}_2\text{-Li}_2\text{S}$  glasses doped with LiBr and LiCl. *Solid State Ion.* **1986**, *18–19*, 368–371. [[CrossRef](#)]
116. Bates, J.B.; Dudney, N.J.; Gruzalski, G.R.; Zuh, R.A.; Choudhury, A.; Luck, C.F.; Robertson, J.D. Fabrication and characterization of amorphous lithium electrolyte thin-films and rechargeable thin-film batteries. *J. Power Sources* **1993**, *43*, 103–110. [[CrossRef](#)]
117. Ryu, J.H.; Kim, E.B.; Lee, J.P.; Lee, S.W. All-Solid-State Batteries Comprising Composite Electrode. US Patent US2022231326 (A1), 21 July 2022.
118. Ryu, J.H.; Kim, E.B.; Lee, J.P.; Lee, S.W. Method of Manufacturing Negative Electrode for All-Solid-State Batteries. US Patent US2022223830 (A1), 14 July 2022.
119. Jung, H.R.; Choi, L.Y.; Han, H.E. Method of Manufacturing Positive Electrode for All-Solid-State Batteries and Positive Electrode for All-Solid-State Batteries Manufactured Using the Same. US Patent US2022190381 (A1), 16 June 2022.
120. Jung, H.R.; Han, H.E.; Hah, H.J. Method of Manufacturing Positive Electrode Mixture for All-Solid-State Batteries and Positive Electrode Mixture for All-Solid-State Batteries Manufactured Using the Same. US Patent US2022181605 (A1), 9 June 2022.
121. Takara, Y.; Takano, R. Solid Electrolyte Ceramic and Solid-State Battery. Patent WO2022107801 (A1), 27 May 2022.
122. Takano, R. Solid Electrolyte Ceramic and Solid-State Battery. Patent WO2022107826 (A1), 27 May 2022.
123. Takara, Y.; Takano, R. Solid Electrolyte Ceramic and Solid-State Battery. Patent WO2022107824 (A1), 27 May 2022.
124. Terai, K.; Kondo, K.; Makino, T.; Sato, A.; Higuchi, H. Sulfide Solid Electrolyte Glass Ceramic and Manufacturing Method for Same. Patent WO2022075471 (A1), 14 April 2022.
125. Fang, Z.; Fu, B.; Xu, Z.; Wu, M. Modified Sodium Ion Solid Electrolyte Ceramic Material with NASICON Type Structure as well as Preparation Method and Application of Modified Sodium Ion Solid Electrolyte Ceramic Material. Patent CN114349494 (A), 15 April 2022.
126. Armand, M. The history of polymer electrolytes. *Solid State Ion.* **1994**, *69*, 309–319. [[CrossRef](#)]
127. Zhang, Q.; Liu, K.; Ding, F.; Liu, X. Recent advances in solid polymer electrolytes for lithium batteries. *Nano Res.* **2017**, *10*, 4139–4174. [[CrossRef](#)]
128. Ha, A.R.; Seong, J.Y.; Kim, Y.-G.; Song, I.W.; Min, H.-S.; Yoon, Y.S.; Kim, Y.-S.; Noh, S.W.; Jang, Y.J.; Lee, S.H.; et al. Cathode Active Material Comprising Ternary Oxide-Containing Coating for all-Solid-State Batteries and Method of Manufacturing Same. Patent CN114122343 (A), 1 March 2022.
129. Ha, Y.K.; Choo, K.C.; Lim, D.H.; Oh, B.H.; Im, H.M. Composite Polymer Solid Electrolyte and Manufacturing Method Thereof. Patent KR20220023731 (A), 2 March 2022.
130. Lyu, P.; Zou, X.; Zhang, D.; Xie, S.; Chen, X.; He, Y. Preparation Method of Polymer Solid Electrolyte Based on Lithium Metal Battery. Patent CN114221038 (A), 22 March 2022.
131. Shang, D.; Wang, Y. Polymer Solid Electrolyte and Preparation Method and Application Thereof. Patent CN114171789 (A), 11 March 2022.
132. Yang, C.C.; Wu, Y.X.; Kumlachew, Z.W. Method for Fabrication of Hybrid Solid Electrolyte Membrane, and All-Solid-State Lithium Battery including the Hybrid Solid Electrolyte Membrane. Patent JP2022029430 (A), 17 February 2022.
133. Ha, Y.K.; Choo, K.C.; Lim, D.H. Hybrid Solid Electrolyte Separator Using Inorganic Fiber and Secondary Battery Using the Same. Patent KR20210146201 (A), 3 December 2021.
134. Kim, H.S.; Kim, M.Y.; Jeon, S.H.; Ban, H.J.; Lim, J.; Lee, J.H. All Solid Lithium Secondary Battery Having High Voltage Stability Comprising Sulfide Based and Oxide-Based Hybrid Solid Electrolyte and Method of Preparing Same. Patent KR20210058101 (A), 24 May 2021.
135. Fraunhofer ISI. *Solid-State Battery Roadmap 2035+*; Fraunhofer ISI: Karlsruhe, Germany, 2022.

**Disclaimer/Publisher’s Note:** The statements, opinions and data contained in all publications are solely those of the individual author(s) and contributor(s) and not of MDPI and/or the editor(s). MDPI and/or the editor(s) disclaim responsibility for any injury to people or property resulting from any ideas, methods, instructions or products referred to in the content.